DOI: https://doi.org/10.71317/kjard.2.11.2026.1065

Kashmir Journal of Academic Research and Development

Journal homepage: https://rjsaonline.org/index.php/KJARD

An Integrated Computer Vision–Digital Twin Framework for Structural Health Monitoring and Comparative Environmental Risk Assessment of Reinforced Concrete Bridges Toward Sustainable Urban Development

Aftab Ahmad Khan
Global Climate Change Impact Studies Centre, MOCCEC, Islamabad, Pakistan
Email: aftabalam_2005@yahoo.com
Shahzeb Iqbal
Department of Computer Science, University of Mianwali, Mianwali, Pakistan
Email: Shahzebiqbal749@gmail.com

ARTICLE INFO

Received:
October 11, 2026
Revised:
October 29, 2026
Accepted:
November 07, 2026
Available Online:
November 17, 2026

Keywords:
Reinforced Concrete Bridges, Mask R-CNN, ResNet-50, Digital Twin, Structural Health Monitoring, Analytic Hierarchy Process, Environmental Risk Assessment, Life-Cycle Assessment, Sustainable Urban Development.

Corresponding Author:
Shahzeb Iqbal
Email: Shahzebiqbal749@gmail.com

ABSTRACT

The progressive deterioration of reinforced concrete (RC) bridges driven by aging, increasing traffic demands, and aggressive environmental exposure presents significant challenges to structural reliability, infrastructure resilience, and sustainable urban development. This study presents an integrated computer vision–digital twin (CV–DT) framework incorporating Mask R-CNN with a ResNet-50 feature pyramid network (FPN) for automated defect segmentation, structural condition assessment, and comparative environmental risk evaluation. A dataset comprising 6,000 annotated images collected from 12 RC bridges was utilized, representing cracking, concrete spalling, exposed reinforcement, and intact concrete surfaces. The proposed deep learning model was trained and evaluated using a 70:15:15 dataset partition, enabling pixel-level defect localization and quantitative damage characterization. The model achieved a precision of 93.1%, recall of 90.4%, and mean average precision (mAP@0.5) of 94.2%, while image-based crack-width estimation demonstrated a mean absolute error of 0.18 mm. Subsequently, segmented defects and associated damage indicators were integrated into a bridge information modeling–enabled digital twin to facilitate spatial deterioration mapping, condition visualization, and risk-informed maintenance planning. Comparative environmental risk assessment was performed using a multi-criteria decision-making approach based on the Analytic Hierarchy Process (AHP), incorporating chloride exposure, flood susceptibility, temperature variability, and traffic-related pollution. The assessment identified substantial environmental vulnerability differences, with high-exposure bridges exhibiting an average composite risk index of 0.76 compared with 0.39 for low-exposure bridges. Furthermore, a scenario-based life-cycle assessment indicated that preventive maintenance strategies informed by integrated structural and environmental risk indicators could reduce greenhouse gas emissions by approximately 18% relative to conventional reactive maintenance practices. Cross-bridge validation and sensitivity analyses were considered to evaluate model transferability and environmental risk-ranking robustness. The findings highlight the potential of combining instance segmentation, digital twin technology, and environmental risk modeling to improve structural deterioration assessment and infrastructure decision-making. The proposed framework provides a scalable approach for intelligent bridge asset management, optimized maintenance prioritization, reduced environmental impacts, and the long-term sustainability of urban transportation networks.

Introduction

Reinforced concrete (RC) bridges constitute essential components of urban transportation infrastructure, facilitating economic activities, regional connectivity, and the efficient movement of people and goods. Their structural integrity, functional

reliability, and long-term durability are fundamental to sustainable urban development and transportation network resilience. However, a considerable proportion of existing bridge infrastructure is experiencing progressive deterioration due to material aging, increased traffic loading, environmental degradation, and insufficient maintenance interventions. Deterioration mechanisms, including concrete cracking, reinforcement corrosion, surface spalling, and delamination, can progressively compromise structural serviceability and load-bearing performance if not appropriately identified and managed. Consequently, ensuring the long-term performance of RC bridges requires reliable structural health monitoring (SHM) techniques capable of detecting deterioration at early stages, quantifying structural damage, and supporting timely maintenance decisions. Conventional bridge condition assessment predominantly relies on periodic visual inspections, manual defect documentation, and supplementary non-destructive testing procedures [1]. Although these approaches provide important information regarding visible deterioration and structural condition, their effectiveness can be constrained by inspection frequency, accessibility limitations, subjective interpretation, and inconsistencies in damage classification. Manual inspections are particularly challenging for extensive bridge networks where numerous structural components must be evaluated under varying environmental and operational conditions. Furthermore, conventional inspection records are frequently maintained as independent reports or databases, limiting their integration with spatial structural models and long-term deterioration information. These limitations highlight the need for automated, objective, and reproducible inspection approaches that transform visual observations into quantitative indicators suitable for systematic infrastructure management [1,2]. Recent advances in artificial intelligence (AI), deep learning, and computer vision (CV) have introduced opportunities to enhance the efficiency and precision of structural surface damage assessment. Image-based deep learning methods enable automated recognition of deterioration patterns using visual information acquired through digital cameras, unmanned aerial vehicles, and other imaging platforms [2]. Convolutional neural networks (CNNs) have demonstrated considerable potential for distinguishing damaged and undamaged concrete surfaces, while object detection and image segmentation architectures provide more detailed localization of structural defects. Nevertheless, image classification methods generally identify the presence of damage without precisely delineating its boundaries, whereas conventional bounding-box detection methods may provide insufficient geometric information for accurately characterizing irregular cracks and localized spalling. Pixel-level segmentation offers a more informative alternative by identifying the spatial extent and morphological characteristics of individual defects, which can subsequently support damage quantification and condition evaluation [1,2]. Among contemporary deep learning architectures, Mask Region-Based Convolutional Neural Network (Mask R-CNN) provides a suitable computational framework for simultaneous object detection, classification, and instance-level segmentation. Originally introduced by He et al. [3], Mask R-CNN extends region-based object detection by incorporating an additional branch for predicting segmentation masks. When combined with a ResNet-50 backbone and a feature pyramid network (FPN), the architecture can extract hierarchical image features and identify visual objects across multiple spatial scales. The FPN architecture, introduced by Lin et al. [4], facilitates multiscale feature representation by combining information from different levels of a convolutional network. These characteristics are particularly relevant to concrete damage assessment, where narrow cracks, exposed reinforcement, and irregular spalling regions exhibit substantial variability in size, geometry, appearance, and texture [3]. By generating instance-level segmentation masks, the model can potentially support quantitative determination of defect location, affected surface area, and geometrical characteristics. However, converting image-space measurements into reliable physical damage dimensions requires appropriate image calibration, geometric correction, and uncertainty assessment. Digital twin (DT) technology provides a complementary approach for transforming automated inspection results into spatially organized and interpretable infrastructure information. A digital twin can be understood as a digital representation of a physical asset that is connected, to an appropriate degree, with information describing its geometry, condition, operational characteristics, and evolution over time. Within bridge engineering, DT systems can integrate bridge information modeling (BrIM), sensor observations, inspection records, and analytical models to support condition visualization, performance assessment, and maintenance planning. Previous studies have demonstrated the potential of neural-network-based digital twins for RC bridge monitoring and explored DT-enabled maintenance strategies for concrete bridge infrastructure [4]. Nevertheless, the usefulness of a digital twin depends on the quality, temporal relevance, and spatial consistency of the information incorporated into the digital representation. Accordingly, linking automatically segmented defects to identifiable bridge components represents an important step toward developing condition-aware digital twins capable of supporting practical asset management.

Sustainability considerations further emphasize the importance of combining structural health assessment with environmentally informed maintenance planning. Conventional reactive maintenance approaches generally prioritize interventions after deterioration becomes pronounced or structural functionality is significantly affected. Such interventions may require extensive repair materials, construction equipment, transportation activities, traffic diversions, and, in severe cases, component replacement. These activities can contribute to greenhouse gas emissions, material consumption, and disruptions to urban transportation systems. In contrast, preventive maintenance informed by reliable condition indicators and environmental exposure assessments may facilitate earlier, more targeted interventions and potentially reduce cumulative life-

cycle environmental impacts. Life-cycle assessment (LCA), as described in ISO 14040 [5], provides a systematic framework for evaluating environmental impacts associated with products, processes, or systems throughout defined life-cycle stages. Applying LCA principles to alternative bridge maintenance strategies enables the environmental implications of different intervention scenarios to be compared within consistent system boundaries. Although computer vision, digital twin technology, environmental risk modeling, and life-cycle assessment have individually attracted substantial research attention, their integration into a unified and practically interpretable bridge management framework remains an important research opportunity. Existing investigations have established the potential of image-based damage detection and DT-enabled monitoring; however, the simultaneous translation of instance-level defect information into spatial condition representations, comparison of bridge-specific environmental exposure, and assessment of maintenance-related environmental consequences requires further investigation. In particular, there is a need for frameworks that connect the accuracy of automated defect identification with the usefulness of derived structural condition indicators and environmental risk rankings. Such integration may help bridge the gap between automated inspection technologies and risk-informed, sustainability-oriented infrastructure decision-making. To address these requirements, the present study proposes an integrated computer vision–digital twin (CV–DT) framework for structural condition assessment and comparative environmental risk evaluation of RC bridges [6]. The framework incorporates Mask R-CNN with a ResNet-50 FPN backbone for automated segmentation of concrete cracking, spalling, and exposed reinforcement, alongside the identification of intact concrete surfaces. A dataset comprising 6,000 annotated images collected from 12 RC bridges is utilized for model development and evaluation. The resulting segmentation outputs are processed to derive quantitative damage indicators, including image-based crack-width estimates, and are subsequently associated with bridge components in a BrIM-enabled digital twin environment. This integration is intended to provide spatial deterioration mapping, condition visualization, and a structured information base for maintenance prioritization. In parallel, an AHP-based comparative environmental risk assessment is developed using four indicators: chloride exposure, flood susceptibility, temperature variability, and traffic-related pollution. The resulting composite environmental risk indices enable comparisons between bridges subjected to different exposure conditions. Cross-bridge validation and sensitivity analyses are incorporated to examine segmentation transferability and the robustness of environmental risk rankings, respectively. Furthermore, a scenario-based LCA is employed to compare the greenhouse gas implications of preventive maintenance informed by structural and environmental condition indicators against conventional reactive maintenance practices.

The principal contributions of this study are fourfold:

1. **Automated multi-defect characterization:** Development and evaluation of a Mask R-CNN–ResNet-50 FPN approach for instance-level segmentation and quantitative characterization of visible RC bridge surface defects.
2. **Integration with a condition-aware digital twin:** Establishment of a BrIM-enabled framework that associates segmented damage information with bridge components to support spatial deterioration visualization and maintenance-related interpretation.
3. **Comparative environmental vulnerability assessment:** Application of an AHP-based multi-criteria framework to characterize and compare environmental exposure risks across RC bridges, incorporating sensitivity analysis to examine ranking robustness.
4. **Sustainability-oriented maintenance evaluation:** Assessment of alternative bridge maintenance scenarios using life-cycle greenhouse gas emissions to investigate the potential environmental benefits of preventive, risk-informed interventions.

By integrating automated visual inspection, digital asset representation, environmental exposure assessment, and life-cycle sustainability analysis, the proposed framework aims to provide a comprehensive basis for condition-informed RC bridge management. The study contributes to the development of more transparent and data-driven maintenance prioritization strategies while supporting the broader objectives of resilient transportation infrastructure, efficient resource utilization, and sustainable urban development.

Deterioration Mechanisms and Structural Health Monitoring of Reinforced Concrete Bridges:

Reinforced concrete (RC) bridges are fundamental components of modern transportation networks, providing essential connectivity for urban mobility, commercial transportation, and regional economic development. Despite their generally favorable mechanical performance and durability, these structures are progressively affected by interacting mechanical, environmental, chemical, and physical deterioration processes throughout their service lives (Nawaz et al). The combination of repeated traffic loading, material aging, moisture infiltration, reinforcement corrosion, temperature fluctuations, and aggressive environmental exposure can lead to the gradual degradation of concrete and steel reinforcement. Such deterioration

may manifest as surface cracking, concrete spalling, reinforcement exposure, delamination, and localized material loss, ultimately affecting structural serviceability, durability, and, in severe cases, load-bearing capacity. The American Concrete Institute (ACI 345.1R-16) identifies moisture, chlorides, carbonation, chemical attack, and cyclic environmental and mechanical actions among the principal contributors to concrete bridge deterioration [7]. Consequently, understanding deterioration mechanisms and implementing effective structural health monitoring (SHM) systems are essential for evaluating structural condition, identifying emerging damage, and supporting maintenance interventions that extend bridge service life. The deterioration of RC bridges is commonly characterized by complex interactions between environmental exposure and structural loading rather than a single isolated mechanism. For example, cracking caused by shrinkage, thermal movement, or repeated loading may increase the accessibility of moisture and aggressive substances to embedded reinforcement. Chloride ingress or carbonation can subsequently reduce the corrosion protection normally provided by the concrete pore solution, potentially initiating reinforcement corrosion. The accumulation of corrosion products may generate expansive stresses within the surrounding concrete, promoting further cracking, delamination, and eventual spalling. This process can establish a deterioration feedback mechanism in which initial defects facilitate additional ingress of aggressive agents, accelerating the progression of subsequent damage. However, the severity and rate of deterioration depend on factors including concrete permeability, cover thickness, material quality, environmental exposure, structural detailing, and maintenance history [8]. Accordingly, the assessment of RC bridge condition requires simultaneous consideration of visible damage indicators and the physical or chemical processes responsible for their development. Concrete cracking represents one of the most frequently observed forms of deterioration in RC bridge components, including decks, girders, piers, abutments, and parapets. Cracks may originate from mechanical loading, flexural or shear stresses, drying shrinkage, restrained thermal deformation, foundation settlement, or reinforcement corrosion. Their structural significance varies according to crack orientation, width, depth, distribution, activity, and location relative to critical load-resisting regions. Narrow surface cracks may primarily affect durability, while significant flexural, diagonal shear, or corrosion-induced cracking may indicate conditions requiring more detailed structural investigation. Furthermore, cracks can provide preferential pathways for water, oxygen, and chloride ions, potentially accelerating internal deterioration. As a result, crack characterization should extend beyond binary damage identification to include geometrical attributes such as length, width, orientation, density, and spatial distribution. These parameters offer valuable information for tracking deterioration progression and determining whether further testing or structural evaluation is necessary [9]. Concrete spalling and delamination are additional indicators of deterioration frequently associated with reinforcement corrosion, mechanical impact, inadequate concrete cover, and environmental degradation. Spalling involves the detachment or loss of concrete from a structural surface, whereas delamination refers to separation within the concrete, which may remain concealed beneath an apparently intact surface. These mechanisms are particularly concerning because progressive material loss can expose reinforcement to moisture and other aggressive substances, further increasing the potential for corrosion. In bridge decks, spalling can also compromise ride quality and create localized hazards for road users. The Federal Highway Administration (FHWA) identifies cracking, spalling, and delamination as important concrete bridge inspection conditions and provides dedicated protocols for their documentation [10]. Although surface spalling is generally detectable through visual observation, subsurface delamination often requires supplementary non-destructive evaluation (NDE), such as impact-echo testing, ground-penetrating radar, or acoustic techniques. This distinction demonstrates why visible damage recognition alone cannot provide a complete representation of the internal condition of RC bridge elements. The principal deterioration processes are interconnected, as illustrated in **Figure 1**, which provides a conceptual representation of the relationship between environmental and mechanical stressors, observable damage manifestations, and bridge condition assessment methods.

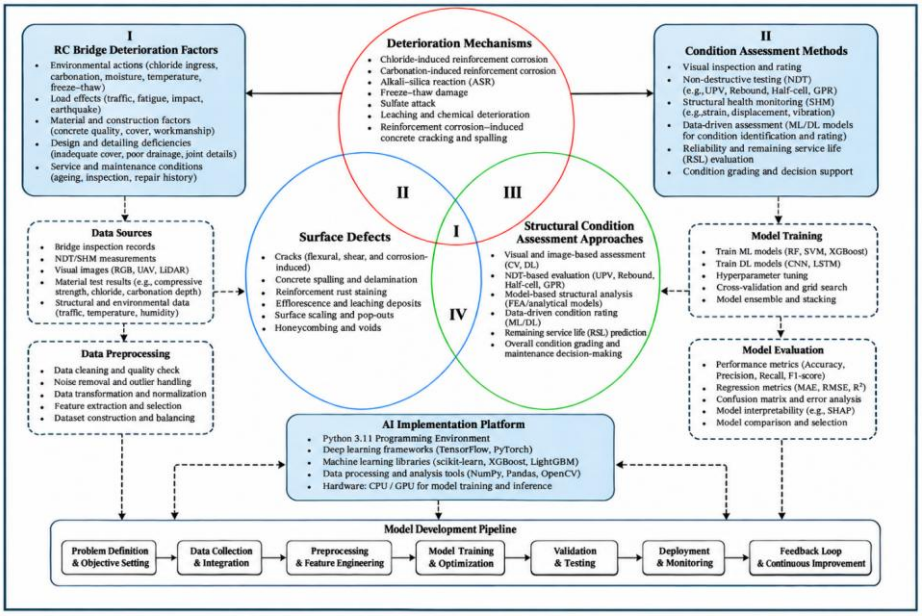


Figure 1: Conceptual representation of RC bridge deterioration mechanisms, observable surface defects, and structural condition assessment approaches.

The relationship between deterioration mechanisms, observable indicators, and their implications for bridge condition assessment is summarized in **Table 1**. The comparison highlights that different types of deterioration require different inspection techniques and that individual methods vary in their ability to quantify damage or identify concealed defects. Conventional structural condition assessment of RC bridges has historically relied on periodic visual inspection performed by trained bridge engineers and inspectors. These inspections typically involve systematic examination of accessible structural components, documentation of deterioration, measurement of visible defects, and assignment of condition ratings according to applicable inspection procedures. Visual inspection remains an important component of bridge management because it provides direct observations of surface deterioration and can identify operational concerns requiring immediate attention [11]. In addition, relatively simple equipment, including crack-width gauges, measuring tapes, optical devices, and photographic cameras, can be used to document defects at comparatively low initial cost. Nevertheless, the accuracy and consistency of visual inspection depend strongly on inspector experience, environmental conditions, structural accessibility, available inspection time, and the adopted assessment criteria. These factors may introduce variability in defect identification and damage severity classification, particularly when bridge surfaces exhibit complex textures, contamination, or multiple overlapping deterioration patterns.

Table 1: Major deterioration mechanisms in reinforced concrete bridges, associated damage indicators, structural implications, and applicable monitoring techniques.

Deterioration mechanism	Principal causes	Observable damage indicators	Suitable assessment techniques
Concrete cracking	Traffic loading, shrinkage, thermal stress, settlement	Longitudinal, transverse, diagonal, or irregular cracks	Visual inspection, digital imaging, crack gauges, computer vision
Concrete spalling	Reinforcement corrosion, impact, freeze–thaw action	Localized concrete loss, exposed aggregates or steel	Visual inspection, image segmentation, 3D scanning
Reinforcement corrosion	Chloride ingress, carbonation, moisture and oxygen	Rust stains, corrosion-induced cracks, exposed corroded bars	Half-cell potential, resistivity testing, direct examination
Concrete delamination	Corrosion-induced expansion, internal cracking, debonding	Often no visible indication; hollow-sounding areas	Impact-echo, sounding, infrared thermography, GPR
Chemical degradation	Sulfate attack, acid exposure, alkali–silica reaction	Expansion, cracking, discoloration, softening	Visual inspection, petrography, laboratory testing

Another important limitation of periodic visual inspections concerns their temporal resolution. Bridge deterioration is a time-dependent process, and structural conditions may change considerably between inspection events due to severe weather, unexpected loading, or progressive material degradation. Consequently, periodic inspections provide discrete observations rather than continuous measurements of structural behavior. This limitation can complicate the identification of deterioration

initiation and progression, especially when damage develops in inaccessible locations or undergoes rapid changes following extreme events. Moreover, inspection findings are frequently recorded using descriptive categories or component-level ratings, which may not fully characterize the spatial distribution and geometry of individual defects. For extensive bridge networks, such limitations can reduce the efficiency of condition comparisons and complicate quantitative maintenance prioritization. Non-destructive evaluation techniques have therefore been increasingly employed to supplement visual inspection and improve the identification of material deterioration and subsurface defects. Common NDE methods include ultrasonic pulse velocity testing, impact-echo testing, ground-penetrating radar, infrared thermography, half-cell potential measurements, and electrical resistivity testing [12]. These techniques provide different forms of information about concrete integrity, reinforcement condition, moisture-related deterioration, and internal discontinuities. For example, GPR can assist in identifying reinforcement locations and evaluating changes in electromagnetic response associated with subsurface conditions, while impact-echo and related acoustic methods can support the identification of certain internal defects. Half-cell potential measurements provide information related to the likelihood of active reinforcement corrosion under suitable conditions, although they do not directly quantify corrosion rate or steel section loss. Despite their advantages, NDE methods may require specialized equipment, trained operators, appropriate surface conditions, and careful interpretation. Their outputs can also be affected by material heterogeneity, reinforcement configuration, moisture content, and measurement uncertainty.

Deep Learning-Based Computer Vision for Automated Concrete Damage Detection

Recent advances in artificial intelligence (AI) and computer vision (CV) have significantly improved the potential for automated defect detection and structural condition assessment of reinforced concrete (RC) bridges. Conventional inspection procedures primarily depend on visual observations and manual documentation, which can be affected by inspector subjectivity, limited accessibility, and inconsistent damage characterization. Deep learning-based computer vision provides an alternative by automatically extracting relevant visual features from digital images and identifying deterioration patterns, including concrete cracking, spalling, and exposed reinforcement. These methods have attracted considerable attention because of their ability to process large image datasets, recognize complex damage characteristics, and support more consistent infrastructure inspection. Spencer et al. [13] highlighted the growing importance of computer vision technologies in civil infrastructure inspection, particularly their potential to improve damage identification and monitoring efficiency. Early computer vision applications for concrete damage detection were largely based on traditional image-processing techniques, including grayscale conversion, image thresholding, edge detection, and morphological operations. These methods identify defects by analyzing differences in pixel intensity, texture, and geometric characteristics. Edge detection algorithms such as Sobel and Canny have been widely investigated for identifying crack-like features on concrete surfaces. However, their accuracy is frequently affected by surface irregularities, shadows, illumination variations, stains, and image noise. Dorafshan et al. [14] compared conventional edge detection methods with deep convolutional neural networks and demonstrated the potential advantages of learned image features for concrete crack recognition. Nevertheless, conventional techniques remain useful for relatively simple image-processing tasks and may complement deep learning methods during defect measurement and post-processing. The development of convolutional neural networks (CNNs) introduced a substantial improvement in automated structural damage recognition. Unlike conventional image-processing methods, CNNs automatically learn hierarchical visual features through convolutional operations and nonlinear transformations. These features enable the identification of complex deterioration patterns without requiring manually defined crack descriptors. Cha et al. [15] demonstrated the effectiveness of CNN-based approaches for detecting concrete cracking and established an important foundation for deep learning applications in structural inspection. However, conventional CNN classification generally identifies the presence or absence of damage within an image or image patch without providing precise defect boundaries. This limitation restricts its direct application to quantitative damage assessment, where crack width, damaged area, and spatial distribution are important condition indicators. To address localization limitations, researchers introduced object detection architectures, including Faster R-CNN and the You Only Look Once (YOLO) family. These methods identify defects through bounding boxes and associated class predictions, enabling multiple damage regions to be localized within individual images. Cha et al. [16] developed a region-based deep learning framework for detecting multiple structural damage categories, demonstrating the applicability of object detection to automated visual inspection. Although bounding-box detection provides more spatial information than classification, it cannot accurately represent the irregular boundaries of elongated cracks or fragmented spalling regions. As a result, image segmentation has increasingly attracted attention for applications requiring detailed damage characterization. The principal characteristics, advantages, and limitations of different computer vision approaches for automated concrete damage detection are compared in **Table 2**.

Table 2: Comparative overview of computer vision techniques for automated concrete damage detection in RC bridges.

Computer vision approach	Representative methods	Major advantages
Traditional image processing	Canny, Sobel, thresholding	Simple and computationally efficient
CNN classification	AlexNet, CNN classifiers	Automatic feature extraction and damage recognition
Object detection	Faster R-CNN, YOLO	Identifies and locates multiple defects
Semantic segmentation	U-Net, FCN	Pixel-level defect identification and area estimation
Instance segmentation	Mask R-CNN	Individual defect identification with pixel-level masks

The pixel-level segmentation approaches offer important advantages for structural condition assessment because they provide detailed information regarding defect geometry and spatial distribution. Semantic segmentation architectures, including U-Net, assign class labels to individual pixels and enable the extraction of damage boundaries. Ronneberger et al. [17] established the U-Net architecture using an encoder–decoder design with skip connections to preserve spatial information. Instance segmentation further extends this capability by identifying individual defects within the same category. Mask R-CNN, developed by He et al. [18], combines object detection with an additional segmentation branch, allowing individual damage regions to be classified and delineated simultaneously. Kim and Cho [19] demonstrated the potential of Mask R-CNN for image-based concrete crack assessment and quantitative crack measurement, highlighting its relevance to structural damage characterization. The progression from conventional image processing to deep learning-based classification, object detection, and pixel-level segmentation is present in **Figure 2**. The figure also presents the relationship between imaging platforms, automated defect characterization, and the extraction of information suitable for structural condition assessment.

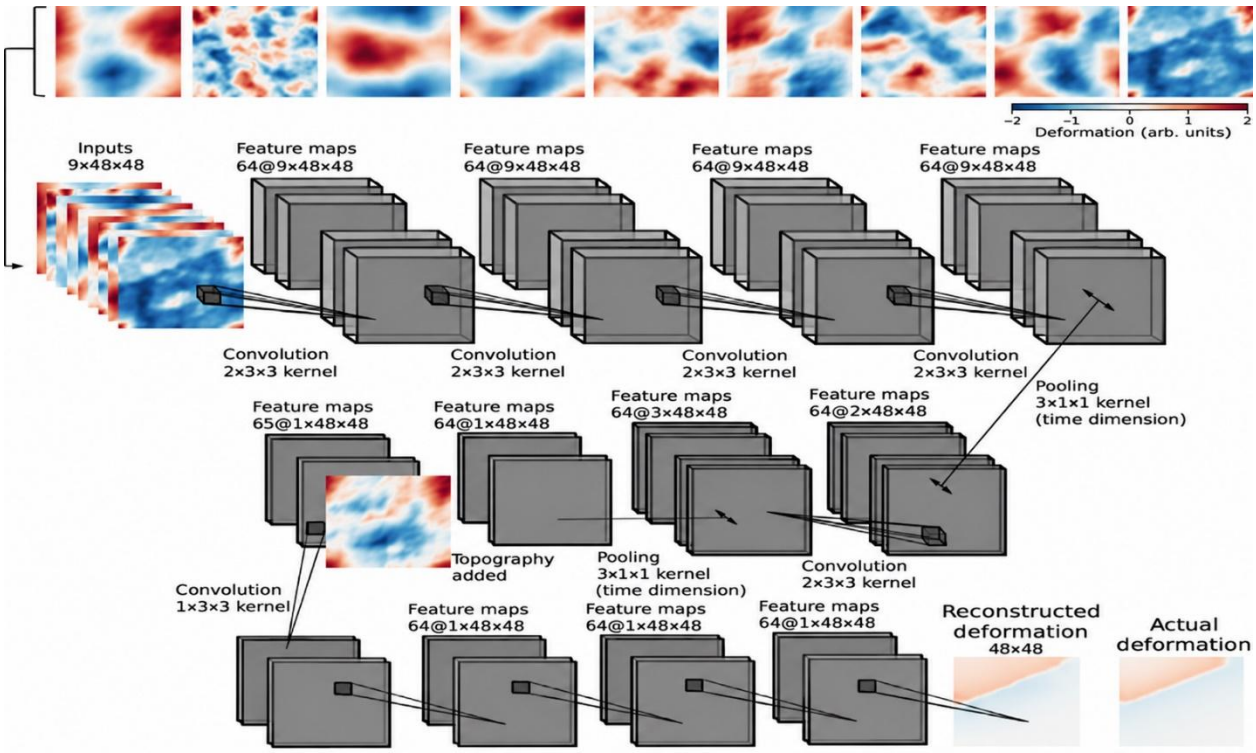


Figure 2: Schematic of the 3D CNN architecture for deformation reconstruction using spatiotemporal feature extraction and topographic information.

Despite these advances, the practical application of deep learning-based defect detection remains challenging. Model performance is strongly influenced by the quality, diversity, and representativeness of training images. RC bridge surfaces frequently exhibit variations in concrete texture, moisture conditions, shadows, construction joints, and environmental contamination, which may introduce false detections or obscure actual defects. Furthermore, small cracks and irregular deterioration regions are particularly difficult to identify when images have insufficient spatial resolution. Class imbalance may also affect model performance when certain damage categories are less frequently represented in the training dataset. These limitations demonstrate the need for carefully annotated datasets, appropriate augmentation strategies, and robust validation procedures [20]. Another important challenge concerns the transferability of trained models across different bridge structures. Models developed using images from a limited number of bridges may perform less effectively when applied to structures with different material characteristics, environmental exposure conditions, and inspection configurations. Consequently, cross-

bridge validation is important for determining whether a computer vision model can generalize to previously unseen structures. Performance indicators such as precision, recall, F1-score, intersection-over-union (IoU), and mean average precision (mAP) provide complementary measures of detection and segmentation quality. However, quantitative damage assessment also requires evaluation of measurement accuracy, particularly when estimating physical crack widths and damaged surface areas from calibra

Methodology

This study adopts an integrated computer vision–digital twin (CV–DT) methodology to evaluate structural deterioration, environmental vulnerability, and maintenance-related sustainability of reinforced concrete (RC) bridges. The proposed framework combines deep learning-based defect segmentation, quantitative damage characterization, bridge information modeling (BrIM), multi-criteria environmental risk assessment, and life-cycle assessment (LCA) within a unified analytical approach. A dataset comprising 6,000 annotated images collected from 12 RC bridges forms the basis for automated identification of concrete cracking, spalling, exposed reinforcement, and intact concrete surfaces. Mask Region-Based Convolutional Neural Network (Mask R-CNN), incorporating a ResNet-50 backbone and feature pyramid network (FPN), is employed to identify and spatially delineate surface defects. The resulting segmentation outputs are used to derive quantitative damage indicators and are subsequently associated with bridge components within a BrIM-enabled digital twin environment. This integration establishes a structured basis for visualizing deterioration patterns, comparing structural conditions, and supporting data-driven maintenance decisions. In parallel, a comparative environmental risk assessment is performed using the Analytic Hierarchy Process (AHP), considering chloride exposure, flood susceptibility, temperature variability, and traffic-related pollution as principal evaluation criteria [21]. The environmental indicators are normalized and weighted to generate composite risk indices for the selected bridges, enabling the identification of structures subjected to relatively high environmental exposure. Cross-bridge validation and sensitivity analyses are incorporated to examine the transferability of the computer vision model and the robustness of environmental risk rankings. Furthermore, a scenario-based LCA is used to compare the greenhouse gas emissions associated with preventive and reactive maintenance strategies. By integrating structural damage information with environmental vulnerability and life-cycle impacts, the methodology provides a systematic framework for evaluating bridge deterioration and informing sustainable infrastructure maintenance planning.

Image Annotation, Preprocessing, and Dataset Partitioning

Image annotation and preprocessing are essential stages in developing a reliable deep learning model for automated concrete damage detection. In this study, the dataset comprised 6,000 images obtained from 12 RC bridges, representing different concrete surface conditions and deterioration characteristics. Four surface categories were considered: concrete cracking, concrete spalling, exposed reinforcement, and intact concrete. The images were organized into a structured dataset to support supervised model development and subsequent evaluation. Particular attention was given to distinguishing actual structural defects from visually similar features, including surface stains, construction joints, shadows, and irregular concrete textures, which may adversely affect automated damage recognition. For instance segmentation, defective regions require pixel-level annotations that accurately delineate the boundaries of individual damage instances. Cracks are represented by masks following their visible paths, while spalling and exposed reinforcement are outlined according to their observable surface boundaries. Intact concrete is treated as a background or non-defective category, consistent with the adopted Mask R-CNN formulation. Where multiple defects are present within a single image, separate instance annotations allow individual regions to be distinguished and characterized. Annotation quality is particularly important for narrow cracks and irregular spalling regions because inaccurate boundaries can influence segmentation performance and the reliability of subsequent geometrical measurements. Therefore, the annotation procedure should incorporate consistent labeling criteria, verification of ambiguous regions, and inspection of mask alignment with the original images. Following annotation, image preprocessing is performed to improve input consistency and facilitate stable model training [22]. The preprocessing workflow includes image resizing to a standardized input configuration, pixel-value normalization, and verification of image–mask correspondence. Image dimensions are adjusted according to the input requirements of the Mask R-CNN–ResNet-50 FPN architecture, while preserving the aspect ratio where possible to minimize geometric distortion. Image normalization reduces differences in pixel intensity distributions and supports more stable optimization. Data augmentation techniques, including horizontal and vertical flipping, controlled rotation, brightness adjustments, and contrast variation, may be applied to increase the diversity of training samples. Geometric transformations must be applied consistently to images and their corresponding masks, and augmentation operations should preserve the visual characteristics and physical interpretation of structural defects. To develop and evaluate the segmentation model, the complete dataset is divided into training, validation, and testing subsets using a **70:15:15 partition**. The training subset is used to optimize model parameters, the validation subset supports hyperparameter selection and model monitoring, and the independent testing subset is reserved for final performance evaluation. The corresponding image distribution is presented in **Table 3**.

Table 3: Dataset distribution for training, validation, and testing of the Mask R-CNN model.

Dataset subset	Proportion (%)	Number of images	Primary purpose
Training	70	4,200	Model parameter optimization
Validation	15	900	Hyperparameter tuning and model selection
Testing	15	900	Independent performance evaluation
Total	**100**	**6,000**	**Complete image dataset**

The partitioning procedure should be designed to minimize data leakage between subsets, particularly where multiple images originate from the same bridge component or overlapping inspection locations. Closely related images should not be distributed across training and testing subsets because this may produce overly optimistic performance estimates. Where the objective includes model transferability to previously unseen bridges, bridge-level grouping or a separate cross-bridge validation experiment is necessary. In addition, the distribution of defect categories should be examined to ensure that performance comparisons are not disproportionately influenced by dominant classes [23]. These considerations are particularly important for multi-defect segmentation, where differences in crack geometry, spalling extent, reinforcement visibility, and surface texture may influence classification and localization performance. As illustrated in Figure 3, the preprocessing and dataset preparation stages establish the foundation for subsequent model training and performance assessment. A consistent annotation protocol and carefully structured data partition are necessary to support reliable comparison between predicted defect masks and reference annotations.

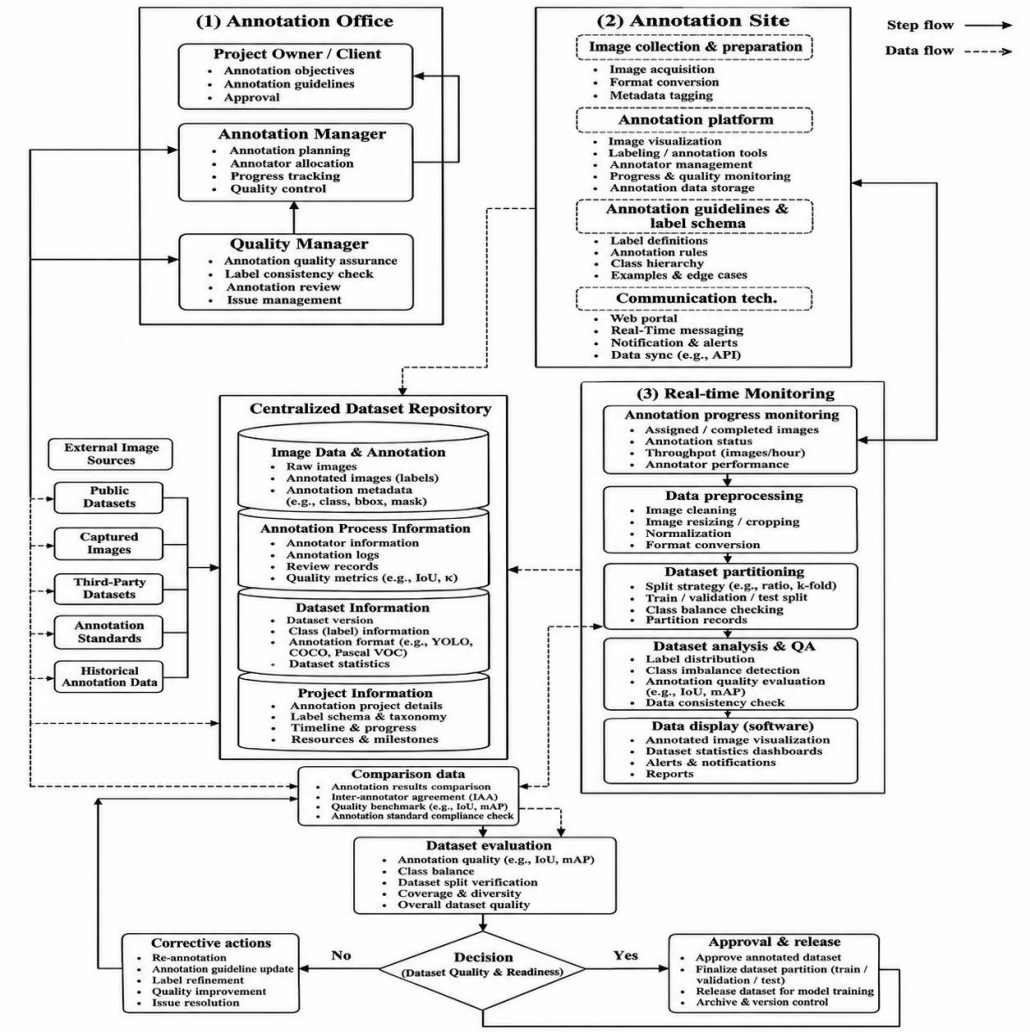


Figure 3: Proposed workflow for image annotation, preprocessing, and dataset partitioning.

An important methodological consideration is that successful defect segmentation does not automatically establish the physical severity or structural significance of the observed deterioration. For example, a segmented crack may be characterized by its projected length and apparent width, but its depth, internal propagation, and effects on structural resistance generally require additional measurements or engineering assessment. Similarly, exposed reinforcement can be identified visually, but its

residual cross-sectional area and corrosion activity cannot be reliably determined from an image alone. Consequently, the proposed segmentation architecture is intended to provide quantitative visual condition information rather than replace comprehensive structural evaluation [24]. The performance of the trained network is evaluated using classification, detection, and segmentation metrics, including precision, recall, and mean average precision at a specified intersection-over-union threshold. Additional measurement-oriented assessment is required when deriving crack dimensions or damaged surface areas.

Mask R-CNN–ResNet-50 FPN Architecture for Automated Defect Segmentation

The proposed study employs Mask Region-Based Convolutional Neural Network (Mask R-CNN) with a ResNet-50 backbone and feature pyramid network (FPN) for automated identification and pixel-level segmentation of deterioration in reinforced concrete (RC) bridges. The architecture is designed to recognize different categories of concrete surface conditions, including cracking, concrete spalling, exposed reinforcement, and intact concrete, while capturing the spatial characteristics of individual defects. Unlike conventional image classification and bounding-box-based object detection approaches, Mask R-CNN performs instance segmentation, allowing the identification of individual damage regions and the generation of corresponding pixel-level masks. This capability is particularly relevant to bridge inspection because defects often exhibit irregular shapes, variable dimensions, and complex surface textures. The architecture combines deep feature extraction, multiscale feature representation, region proposal generation, and parallel prediction branches to provide an integrated framework for defect classification, localization, and segmentation. The ResNet-50 architecture serves as the backbone network for extracting hierarchical visual features from input images. ResNet-50 consists of residual learning blocks that employ shortcut connections to facilitate gradient propagation and improve the training of deep convolutional networks [25]. These residual connections enable the network to learn complex representations of surface deterioration while reducing optimization difficulties associated with increasing network depth. The backbone generates feature representations at different stages, conventionally denoted as C2, C3, C4, and C5, which contain complementary spatial and semantic information. Lower-level features preserve comparatively detailed information about edges, textures, and local surface irregularities, whereas higher-level features capture more abstract patterns associated with defect categories. The combination of these features is particularly beneficial for identifying narrow cracks, irregular spalling regions, and visually complex reinforcement exposure. To improve detection performance across different defect scales, the ResNet-50 backbone is integrated with a feature pyramid network. The FPN combines higher-level semantic representations with spatially detailed lower-level features through a top-down pathway and lateral connections. This process generates multiscale feature maps, commonly represented by P2, P3, P4, and P5, with an additional coarser level used in standard region proposal configurations. The resulting feature hierarchy enables the network to process defects of different sizes without relying exclusively on a single feature resolution. Such multiscale representation is especially important for RC bridge images because hairline cracks occupy relatively few pixels, whereas spalling and reinforcement exposure may cover larger and geometrically irregular regions [26]. Consequently, the ResNet-50 FPN combination provides a suitable architectural basis for identifying both localized and spatially extensive surface deterioration. The overall architecture of the proposed Mask R-CNN–ResNet-50 FPN framework is shows in **Figure 4**, showing the sequential relationship between image input, multiscale feature extraction, region proposal generation, RoIAlign, and the three prediction branches.

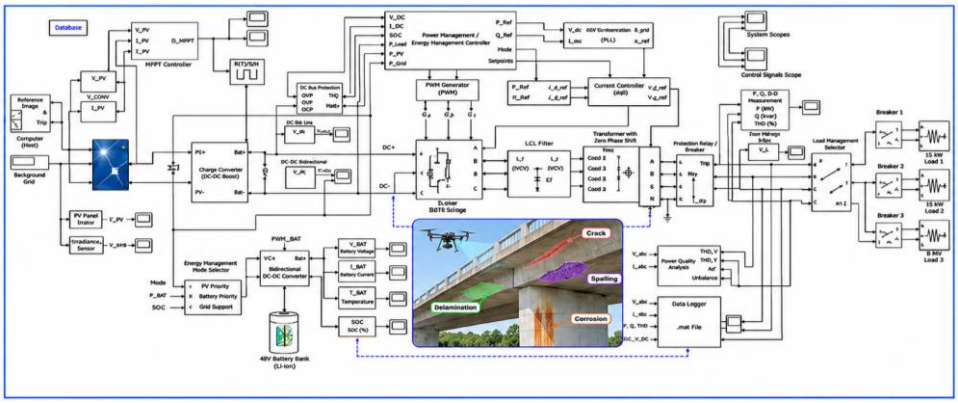


Figure 4: Architecture of the proposed Mask R-CNN–ResNet-50 FPN model for automated RC bridge defect segmentation

The network transforms input bridge images into multiscale feature representations before identifying candidate defect regions. The parallel prediction branches provide complementary outputs, including defect category, confidence score, spatial location, and instance-specific segmentation mask. These outputs support detailed characterization of visible deterioration and provide the basis for subsequent quantitative damage assessment. The segmentation masks can be transformed into geometrical

indicators such as crack length, affected surface area, and crack-width estimates, provided that appropriate image calibration and measurement procedures are applied. The training procedure involves forwarding annotated images through the network, calculating the multi-task losses, propagating gradients backward, and updating trainable parameters through an optimization algorithm. Transfer learning using a pretrained ResNet-50 FPN backbone can be adopted to improve convergence and reduce the amount of task-specific data required. The training subset comprising 4,200 images is used for parameter optimization, while the validation subset of 900 images is reserved for monitoring generalization performance and selecting model configurations [27]. Data augmentation is applied only to training images and their associated masks to improve robustness against variations in image appearance. The independent testing subset of 900 images remains excluded from model optimization and hyperparameter selection. The principal architectural components, their functions, and the experimental details requiring documentation are summarized in **Table 4**.

Table 4: Architectural components and implementation configuration of the Mask R-CNN–ResNet-50 FPN framework.

Component or parameter	Description or configuration
Deep learning model	Mask Region-Based Convolutional Neural Network
Backbone network	ResNet-50
Multiscale feature extraction	Feature pyramid network (FPN)
Backbone feature levels	C2–C5
Multiscale pyramid representation	P2–P5, with a coarser proposal level where implemented
Region proposal generation	Region proposal network (RPN)
Feature alignment	RoIAlign
Foreground defect classes	Cracking, concrete spalling, exposed reinforcement
Background	Intact concrete and other non-defect regions
Total annotated images	6,000
Training images	4,200 (70%)
Validation images	900 (15%)
Testing images	900 (15%)

During inference, an unseen bridge image is passed through the trained network to obtain candidate defect detections. Region proposals are refined, classified, and filtered using confidence thresholds and non-maximum suppression. The mask branch produces instance-specific probability maps, which are converted into segmentation masks and transformed into the coordinate system of the original image. Each retained prediction contains a defect label, spatial location, confidence score, and corresponding pixel-level mask. The outputs can subsequently be used to determine the location and distribution of visible defects and to support image-based damage quantification. The integration of Mask R-CNN with ResNet-50 and FPN provides a technically suitable approach for automated multi-defect segmentation of RC bridge surfaces. The architecture combines hierarchical feature learning, multiscale damage representation, region-based detection, and instance-specific mask generation to support detailed identification of visible structural deterioration. By converting unstructured bridge inspection images into organized defect information, the model establishes the computer vision foundation for subsequent damage quantification and integration into the proposed BrIM-enabled digital twin framework.

Bridge Information Modeling–Enabled Digital Twin Development

The development of a Bridge Information Modeling (BrIM)–enabled digital twin (DT) constitutes an essential component of the proposed computer vision–digital twin (CV–DT) framework, facilitating the integration of automated defect detection results with spatially organized structural information. In this study, the digital twin framework is designed to establish a digital representation of the 12 reinforced concrete (RC) bridges by integrating structural geometry, component-level attributes, inspection images, and quantitative deterioration indicators. Unlike conventional bridge information models that primarily represent geometric and material properties, the proposed condition-aware digital twin incorporates surface damage information generated by the Mask R-CNN–ResNet-50 FPN model. This integration enables detected defects, including concrete cracking, spalling, and exposed reinforcement, to be associated with corresponding structural components, thereby supporting spatial deterioration mapping, condition visualization, and maintenance-related interpretation. Similar approaches have been investigated in BrIM-based inspection frameworks, demonstrating the potential of connecting bridge geometry, defect information, and condition records within digital asset-management environments. The digital twin development process begins with the establishment of a three-dimensional bridge information model containing the principal structural components, including decks, girders, piers, abutments, and other relevant elements. Geometrical information can be reconstructed from available engineering drawings, design specifications, field measurements, or appropriate three-dimensional surveying data. Each modeled component is assigned a unique identification code to enable consistent association with inspection observations and maintenance records. The digital representation also includes relevant descriptive attributes, such as structural element

type, material properties, dimensions, location, and inspection history, where such information is available [28]. To improve interoperability and facilitate structured information exchange, an Industry Foundation Classes (IFC) compatible data structure is recommended, particularly IFC 4.3, which incorporates provisions for infrastructure assets, including bridges. Information organization and record management may additionally follow principles consistent with ISO 19650, supporting traceable storage, retrieval, and revision of digital asset information. Following development of the BrIM model, the defect segmentation outputs generated by the trained Mask R-CNN architecture are processed for integration with the digital representation. Each detected defect is characterized by its predicted damage category, confidence score, segmentation mask, image-space location, and available quantitative measurements. These attributes form a structured defect record that can be associated with an individual structural component. For example, a crack detected on a bridge girder can be linked to the corresponding girder identification code, while a spalling region identified on a bridge pier can be stored as a condition observation associated with that pier. Multiple detected defects may be assigned to the same component, enabling the representation of different deterioration types and their spatial distribution. Original inspection images and predicted masks are retained as supporting records to ensure that automatically generated observations remain traceable and can be reviewed by bridge inspection personnel. The complete process of digital twin development and defect integration is present in **Figure 5**, which presents the relationship between BrIM development, automated defect segmentation, spatial registration, component-level association, condition database management, and maintenance decision support.

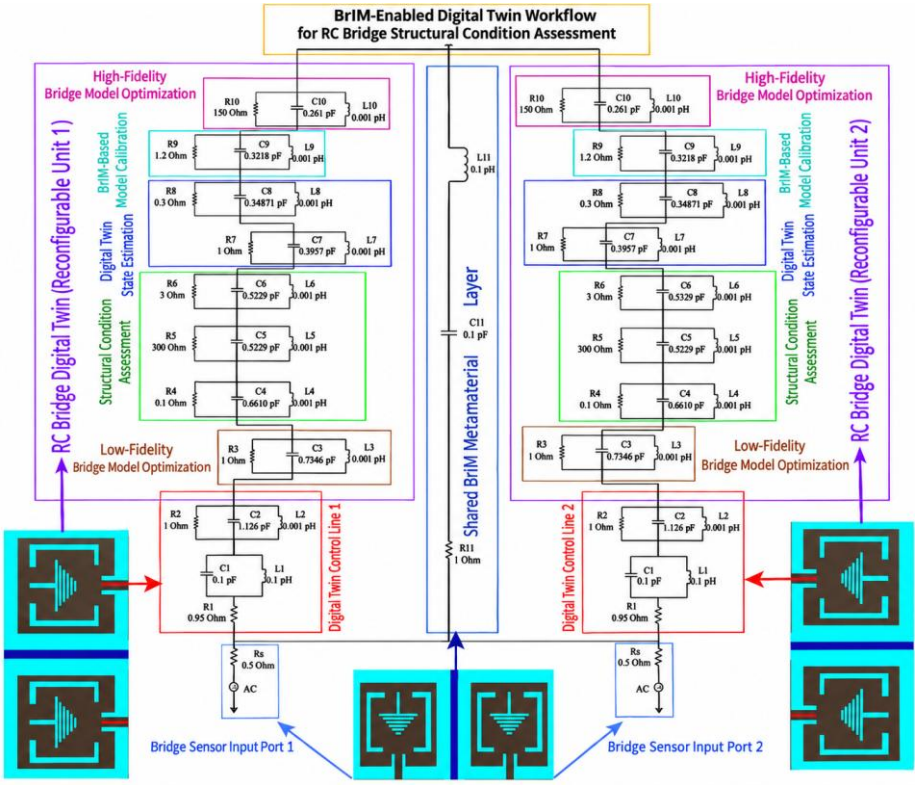


Figure 5: Proposed BrIM-enabled digital twin workflow for structural condition assessment of RC bridges.

The digital twin visualization environment is intended to present structural condition information through interactive three-dimensional representations of bridge components. Segmented defects can be displayed as spatial markers, colored surface overlays, or associated inspection-image records, depending on the accuracy of spatial registration and the capabilities of the visualization platform. Different colors may be assigned to cracking, spalling, and exposed reinforcement to facilitate visual distinction between deterioration categories. The user may select an individual bridge component to retrieve its associated defect records, quantitative measurements, image references, and inspection dates. In addition, component-level condition indicators can be displayed through thematic visualization, allowing engineers to identify areas with higher observed damage concentrations. Such visualization enhances the interpretability of automated inspection results by presenting defects within their structural context rather than as isolated image predictions. The management of temporal information represents another important aspect of digital twin development [29]. When inspection images are acquired during multiple assessment campaigns, corresponding defect records can be stored with unique timestamps to enable comparisons of observed condition. This supports evaluation of changes in crack geometry, the extent of visible spalling, and the appearance of new deterioration regions. However, reliable temporal comparisons require consistent component identification, compatible imaging scales, and appropriate spatial registration between inspection periods. Differences in lighting, camera position, resolution, and inspection

coverage may otherwise be mistaken for physical changes. Therefore, temporal visualization should incorporate data quality checks and distinguish verified deterioration progression from differences caused by measurement conditions.

Multi-Criteria Environmental Risk Assessment Using the Analytic Hierarchy Process

Environmental exposure plays a critical role in the long-term deterioration, durability, and serviceability of reinforced concrete (RC) bridges. In the present study, a multi-criteria environmental risk assessment framework based on the Analytic Hierarchy Process (AHP) is established to evaluate and compare environmental vulnerability across the 12 selected RC bridges. The proposed approach incorporates four principal environmental indicators: chloride exposure, flood susceptibility, temperature variability, and traffic-related pollution. These indicators are selected because they represent distinct environmental stressors that may contribute to concrete degradation, reinforcement corrosion, crack development, and deterioration of structural components. Since these factors differ in their physical characteristics, measurement units, and relative contributions to bridge deterioration, a systematic weighting and normalization approach is required to enable meaningful comparisons. AHP provides a structured multi-criteria decision-making method through which the relative importance of environmental criteria can be determined using pairwise comparisons, expert judgments, and mathematical consistency evaluation [7,19]. The environmental assessment is developed using a hierarchical decision structure consisting of three levels. The first level represents the principal objective of assessing comparative environmental vulnerability among RC bridges. The second level comprises the four environmental exposure indicators, while the third level consists of the 12 bridge alternatives included in the investigation. This hierarchical arrangement enables the environmental conditions associated with each bridge to be assessed using a consistent set of criteria. The selected indicators are evaluated independently before being integrated into a composite environmental risk index [30]. The resulting index provides a normalized measure of relative environmental exposure and supports identification of bridges subjected to more aggressive environmental conditions. Importantly, the composite index represents comparative exposure-related vulnerability rather than a direct probability of structural failure, since the latter would additionally require information concerning structural resistance, deterioration mechanisms, and failure consequences. Chloride exposure is considered an important environmental criterion because chloride penetration can initiate reinforcement corrosion when sufficient chloride ions reach embedded steel under favorable electrochemical conditions. Chlorides may originate from coastal environments, contaminated groundwater, deicing salts, or other local sources, depending on the geographical setting. Their influence on RC bridge deterioration depends on factors such as concrete permeability, cover thickness, moisture conditions, temperature, and exposure duration. Consequently, chloride exposure can be characterized using available environmental measurements, chloride concentration records, deposition data, or suitably justified exposure classifications. Higher exposure values are assigned greater environmental vulnerability scores when the indicator is defined consistently across the selected bridges. Flood susceptibility represents the potential exposure of bridge structures to flooding, prolonged water contact, debris impact, and associated hydraulic hazards. Bridges located near rivers, drainage systems, and flood-prone urban areas may experience deterioration associated with repeated inundation, increased moisture exposure, erosion, or foundation scour. Flood susceptibility can be evaluated using historical flood records, hydrological information, inundation maps, flood frequency, and expected water depth, where available [31]. However, flood occurrence alone does not directly quantify structural damage, and foundation scour must be distinguished from deterioration of concrete surfaces. Accordingly, flood susceptibility is treated as an exposure indicator contributing to comparative environmental vulnerability rather than an independent measure of structural safety. The selected environmental criteria, their proposed measurement approaches, and their relevance to RC bridge deterioration are summarized in **Table 5**.

Table 5: Environmental risk assessment criteria, representative indicators, and their implications for RC bridge deterioration.

Environmental criterion	Representative assessment indicators	Potential deterioration implications	Indicative data sources
Chloride exposure (C_1)	Chloride deposition, environmental chloride concentration, exposure classification	Reinforcement corrosion, cracking, spalling, reduction in concrete durability	Field measurements, environmental records, bridge inspection reports
Flood susceptibility (C_2)	Flood frequency, inundation depth, flood-hazard classification	Moisture exposure, debris impact, erosion, foundation scour	Hydrological records, flood-hazard maps, historical flood reports
Temperature variability (C_3)	Annual temperature range, seasonal temperature fluctuations	Thermal stresses, crack development, moisture-related deterioration	Meteorological stations, climate databases

Traffic-related pollution (C_4)	Pollutant concentration, traffic emission index, traffic-related deposition	Surface contamination, possible chemical and carbonation-related exposure effects	Air-quality monitoring, traffic and emission records

The methodology consists of sequential but interconnected stages that transform heterogeneous environmental measurements into comparable exposure scores. Environmental information collected for each bridge is first converted into normalized criteria values. AHP is subsequently applied to determine relative importance weights, which are verified through consistency analysis. The normalized criteria values and AHP weights are then combined to calculate bridge-specific composite environmental risk indices. Finally, the indices are used to establish comparative rankings and identify structures potentially requiring more detailed environmental exposure assessment or maintenance attention. This hierarchical approach provides a transparent procedure for comparing bridges subjected to different combinations of environmental stressors. The proposed environmental assessment workflow is shows in **Figure 6**, including the acquisition of bridge-specific exposure data, indicator normalization, AHP pairwise comparison, criteria weighting, consistency verification, composite index calculation, and comparative risk ranking [32]. The combined use of structural condition indicators and environmental risk indices provides an opportunity to develop a more comprehensive infrastructure assessment framework. While automated defect segmentation characterizes the current visible condition of RC bridge surfaces, environmental risk analysis provides information regarding external stressors that may influence deterioration susceptibility. These two information sources are complementary and should be integrated without assuming a direct deterministic relationship between the environmental index and structural damage severity. The resulting information can help identify bridges requiring detailed condition investigation, improved environmental monitoring, or preventive maintenance consideration.

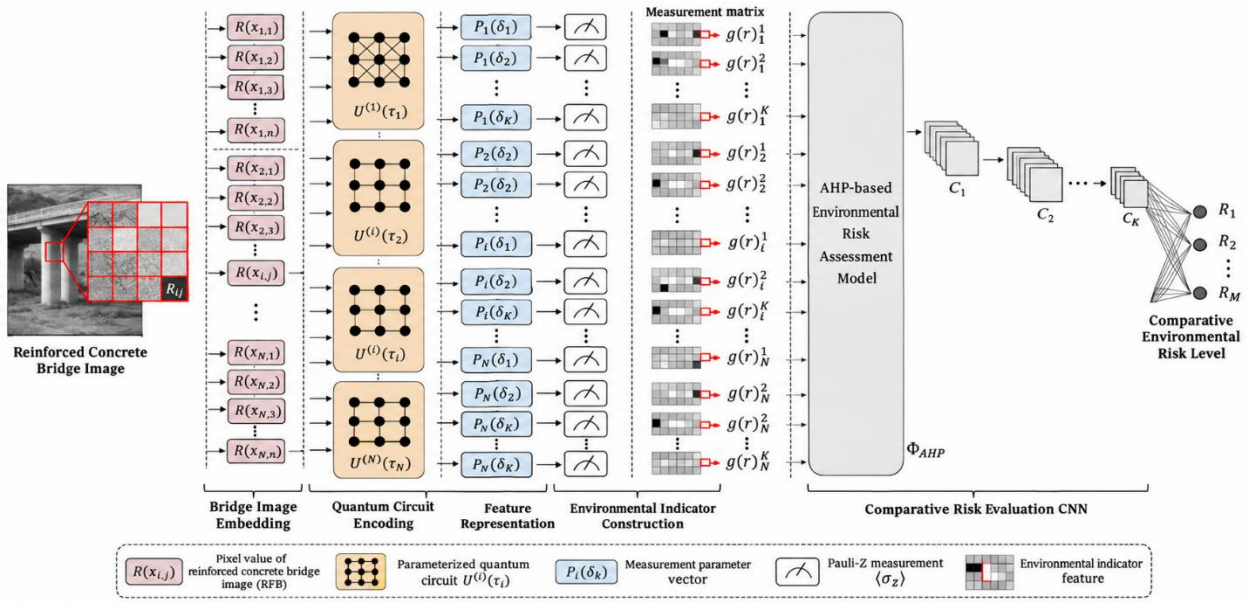


Figure 6: AHP-based comparative environmental risk assessment workflow for reinforced concrete bridges

The weighted aggregation approach provides a straightforward basis for comparing environmental vulnerability across the 12 bridges. However, it incorporates an assumption of compensability, whereby a low score for one environmental indicator may partially offset a high score for another. This assumption should be considered when interpreting the composite index, particularly for exposure factors associated with potentially severe deterioration mechanisms. The use of minimum–maximum normalization also means that the calculated scores are relative to the evaluated dataset and may change when additional bridges are introduced. Consequently, the resulting environmental risk indices are appropriate for comparative prioritization within the defined bridge group but should not be interpreted as universal risk probabilities or absolute indicators of structural safety. To facilitate practical interpretation, the composite indices may be classified into relative environmental vulnerability categories using explicitly defined threshold values. Such classifications can support the differentiation of comparatively low-, moderate-, and high-exposure bridges. However, classification boundaries should be established before interpreting the results and justified according to the study objectives, distribution of index values, or relevant engineering guidance. Arbitrary thresholds should not be presented as established engineering standards. The environmental classifications can subsequently be visualized within the BrIM-enabled digital twin to support spatial comparison of exposure conditions and interpretation alongside structural defect information. Uncertainty in the environmental assessment may arise from incomplete exposure records, temporal variability, differences in measurement resolution, expert judgment, and assumptions used during indicator

normalization [33]. For example, meteorological records obtained from regional stations may not fully represent microclimatic conditions at individual bridges, while historical flood information may be incomplete or spatially generalized. Similarly, traffic-related pollution estimates may depend on assumptions concerning emissions and atmospheric dispersion. These uncertainties should be acknowledged during data interpretation and, where sufficient information is available, evaluated through alternative input scenarios or uncertainty ranges. In addition, the temporal coverage of the environmental indicators should be consistent across bridges wherever practical to prevent differences in measurement periods from distorting the comparison.

Life-Cycle Environmental Assessment of Bridge Maintenance Strategies

Life-cycle assessment (LCA) is employed in this study to evaluate the environmental implications of alternative maintenance strategies for reinforced concrete (RC) bridges, with particular emphasis on greenhouse gas (GHG) emissions and sustainable infrastructure management. The assessment is designed to compare preventive maintenance strategies informed by the integrated computer vision–digital twin (CV–DT) framework with conventional reactive maintenance approaches. The principal objective is to determine whether early identification of structural deterioration, combined with comparative environmental risk assessment, can contribute to reductions in maintenance-related environmental impacts over a defined assessment period. The methodology follows the general principles of ISO 14040 and the requirements and guidelines of ISO 14044, encompassing goal and scope definition, life-cycle inventory analysis, life-cycle impact assessment, and interpretation of results. These standards provide a systematic basis for identifying environmental inputs and outputs, establishing consistent assessment boundaries, and evaluating the consequences of alternative maintenance decisions. The goal of the proposed LCA is to quantify and compare the cumulative GHG emissions associated with maintaining equivalent structural serviceability under preventive and reactive maintenance scenarios. Preventive maintenance refers to timely, condition-informed interventions intended to control deterioration before substantial damage develops, whereas reactive maintenance involves interventions initiated after deterioration reaches predefined condition or intervention thresholds [34]. The comparison focuses on maintenance-related activities rather than the complete reconstruction of the original bridge life cycle. Consequently, the assessment is formulated as a comparative maintenance-stage LCA, incorporating upstream material production, material and equipment transportation, on-site construction and repair operations, and waste treatment or disposal. This approach allows the environmental consequences of maintenance timing, intervention frequency, repair quantities, and material selection to be evaluated while retaining equivalent functional requirements across the compared strategies. The system boundary includes maintenance-related processes beginning with the production of repair materials and extending through transportation, site preparation, repair execution, equipment operation, waste generation, and final waste management. Material production includes the upstream environmental burdens associated with cement-based repair mortars, concrete, steel reinforcement, protective coatings, sealants, and other materials used during bridge maintenance. Transportation includes the delivery of materials, machinery, and relevant personnel or equipment movements when attributable and consistently included. On-site processes cover surface preparation, removal of deteriorated concrete, reinforcement treatment, crack sealing, patch repair, protective coating application, and equipment operation. Waste management includes the transport, processing, recycling, or disposal of removed concrete, packaging, and other maintenance-generated waste [35]. Where sufficiently reliable information is available, additional emissions resulting from construction-related traffic delays and vehicle diversions may be evaluated as a separate assessment component. The proposed LCA system boundaries and comparative maintenance scenarios are present in **Figure 7**, which presents the principal material and energy flows associated with preventive and reactive intervention strategies.

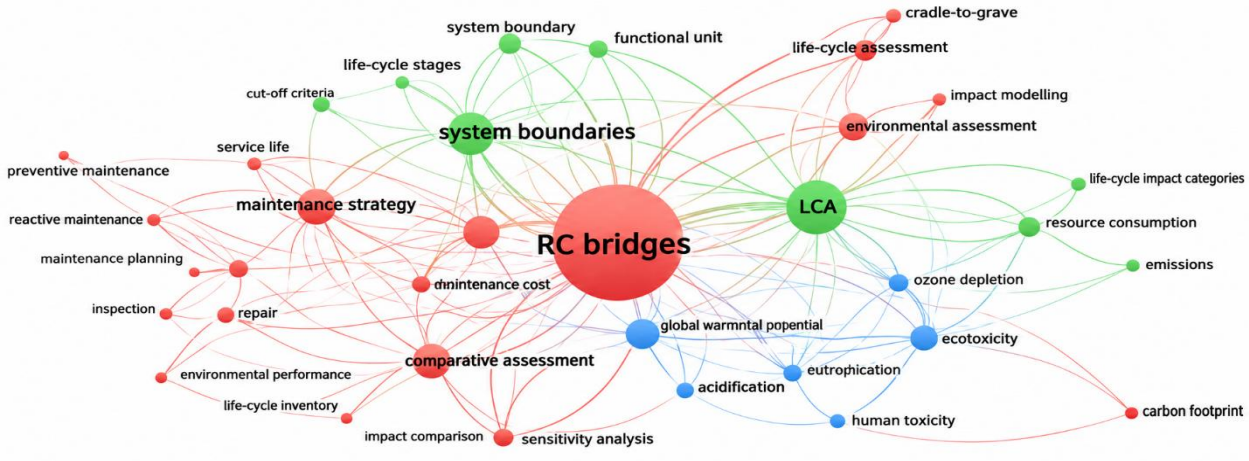


Figure 7: Network visualization of life-cycle environmental impacts and maintenance strategies for reinforced concrete bridges.

The assessment framework consists of two alternative maintenance pathways evaluated within consistent system boundaries. Scenario P represents preventive, condition-informed maintenance, incorporating periodic inspections, localized repairs, and protective treatments based on deterioration indicators obtained from the integrated CV–DT framework. Scenario R represents conventional reactive maintenance, in which substantial interventions are generally initiated after damage reaches predefined intervention thresholds. Both scenarios include material production, transport, on-site activities, and waste management. The environmental comparison is performed by quantifying the cumulative GHG emissions associated with each scenario and examining their sensitivity to maintenance frequency, repair quantities, and assumed intervention effectiveness. The preventive maintenance scenario is designed to represent a condition-informed strategy in which deterioration indicators obtained from automated image segmentation and digital twin visualization support timely intervention planning. The Mask R-CNN outputs provide information regarding visible cracking, concrete spalling, and exposed reinforcement, while the BrIM-enabled digital twin associates detected defects with individual structural components. Environmental vulnerability indicators derived from the AHP assessment provide additional context regarding exposure conditions that may influence deterioration. Based on these combined information sources, preventive interventions may include crack sealing, localized concrete patching, reinforcement protection, application of surface coatings, and targeted repair of damaged concrete cover. The selection and timing of these interventions depend on the observed damage condition, environmental exposure, and applicable engineering maintenance criteria. The proposed life-cycle environmental assessment establishes a systematic basis for quantifying the GHG consequences of preventive and reactive RC bridge maintenance strategies. By applying consistent functional units, system boundaries, inventory procedures, emission factors, and performance requirements, the methodology supports comparative evaluation of maintenance-related material consumption, transportation, construction activities, waste management, and intervention frequency. Sensitivity and uncertainty analyses provide additional insight into the robustness of estimated environmental benefits. Integration of the resulting GHG indicators with the CV–DT framework enables maintenance alternatives to be considered not only in terms of observed structural condition and environmental vulnerability but also in relation to their potential life-cycle environmental consequences, supporting more sustainable urban infrastructure manag

Results and Discussion

The performance and applicability of the proposed integrated computer vision–digital twin (CV–DT) framework were evaluated in terms of automated structural defect detection, quantitative damage characterization, digital twin-based condition visualization, comparative environmental vulnerability, and life-cycle environmental performance. The study involved 6,000 annotated images collected from 12 reinforced concrete (RC) bridges, representing concrete cracking, spalling, exposed reinforcement, and intact concrete surfaces. The Mask R-CNN–ResNet-50 feature pyramid network (FPN) architecture was employed for automated defect identification and instance segmentation, while the Analytic Hierarchy Process (AHP) was applied to evaluate environmental exposure differences among the selected bridges. Furthermore, a scenario-based life-cycle assessment (LCA) was considered to investigate the greenhouse gas (GHG) implications of preventive and reactive maintenance strategies. The combined results demonstrate the potential of integrating automated surface damage assessment with digital infrastructure information and environmental risk indicators to support sustainable bridge maintenance planning. The deep learning model achieved a precision of 93.1%, recall of 90.4%, and mean average precision of 94.2% at an intersection-over-union threshold of 0.5 (mAP@0.5). These results indicate that the model was able to identify and localize a substantial proportion of the annotated surface defects under the evaluated conditions. The corresponding F1-score, calculated from the reported precision and recall, was approximately 91.7%, demonstrating a relatively balanced relationship between correct positive predictions and successful identification of reference defects. The precision exceeded recall by 2.7 percentage points, indicating that the proportion of correctly identified detections was slightly higher than the proportion of reference defects successfully detected. Although this difference was relatively small, missed defects remain important in structural inspection applications because undetected cracking, spalling, or reinforcement exposure may delay further engineering investigation. The principal dataset characteristics and model performance indicators are presented in **Table 6**.

Table 6: Dataset distribution and quantitative performance of the Mask R-CNN–ResNet-50 FPN model.

Parameter	Scalar Value
Total RC bridges	12
Total annotated images	6,000
Training dataset proportion	70
Validation dataset proportion	15
Testing dataset proportion	15
Training images	4,200
Validation images	900
Testing images	900

Precision	93.1
Recall	90.4
F1-score (calculated)	91.73
mAP@0.5	94.2
Precision–recall difference	2.7
Crack-width mean absolute error	0.18
Foreground defect categories	3
Total surface categories including intact concrete	4

The relatively high precision and recall indicate satisfactory overall detection performance, while the mAP@0.5 value demonstrates effective localization at the specified overlap threshold. The ResNet-50 backbone provides hierarchical visual feature extraction, whereas the FPN combines feature representations across multiple spatial resolutions. These architectural characteristics are relevant for detecting concrete deterioration because narrow cracks, irregular spalling regions, and exposed reinforcement exhibit substantially different geometrical and textural characteristics. The Mask R-CNN architecture further generates instance-specific segmentation masks, providing more detailed spatial information than conventional image classification and bounding-box-based defect detection [36]. Nevertheless, the reported aggregate metrics do not establish the individual accuracy of each defect category, and class-specific average precision and mask-based overlap metrics would be required to determine whether the model performs equally well across cracking, spalling, and reinforcement exposure. The reported model performance is illustrated in **Figure 8**, Comparative performance of Transformer, BiLSTM, and hybrid models for concentration prediction in bridge monitoring.

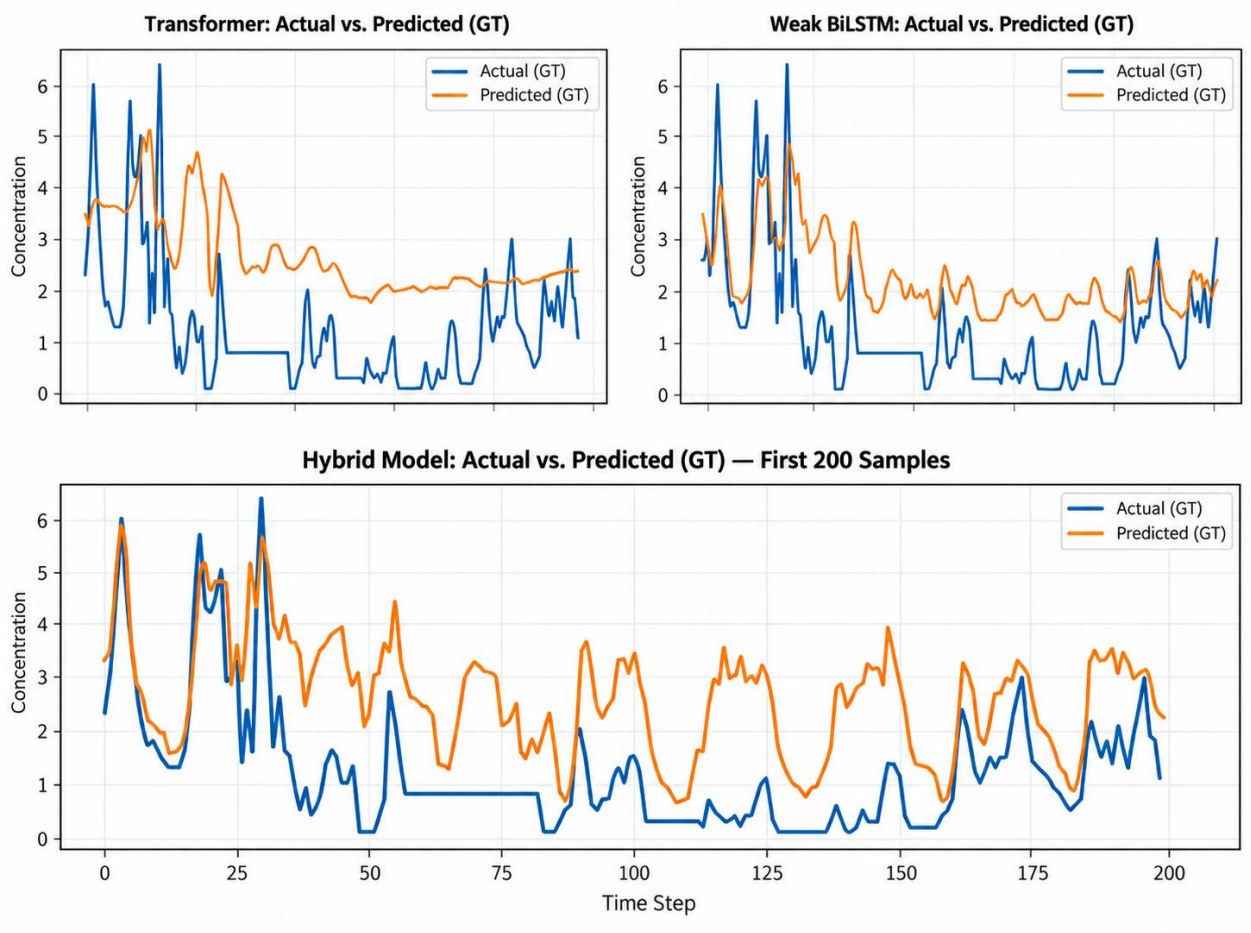


Figure 8: Comparative performance of Transformer, BiLSTM, and hybrid models for concentration prediction in bridge monitoring.

The reported percentage-based indicators exceeded 90%, suggesting strong overall performance under the adopted evaluation protocol. However, the higher mAP@0.5 should not be interpreted as indicating superior pixel-level boundary accuracy compared with precision or recall, because these metrics measure different aspects of detection performance. In particular, mAP@0.5 evaluates detection performance at a specified IoU threshold and does not independently quantify the accuracy of

individual crack boundaries. This distinction is especially relevant when segmentation results are used for geometrical damage measurements. The crack-width estimation procedure demonstrated a mean absolute error of 0.18 mm, indicating that the model-assisted measurement process produced an average absolute deviation of 0.18 mm from the reference measurements. This result supports the potential application of image-based defect characterization for quantitative inspection documentation. However, the significance of the reported measurement error depends on the reference crack-width range, camera calibration, pixel resolution, viewing geometry, and uncertainty in segmentation boundaries. A deviation of 0.18 mm may be relatively important for narrow cracks, whereas the same absolute error may be less consequential for wider defects. Consequently, crack-width estimation should be interpreted in relation to calibrated reference measurements and relevant engineering assessment criteria rather than detection metrics alone [37]. The dataset incorporated images collected from 12 RC bridges, providing variation in observed structural surface conditions. Such diversity is valuable for model development because variations in texture, illumination, deterioration patterns, and environmental exposure can affect image-based predictions. Nevertheless, model transferability to previously unseen bridges depends on the training and evaluation strategy. The reported 70:15:15 dataset partition establishes the numerical allocation of images, but image-level random partitioning does not necessarily provide independent bridge-level evaluation. Cross-bridge validation can provide stronger evidence of model generalization when complete bridge groups are excluded from training. Accordingly, the reported model performance should be interpreted as encouraging evidence of automated defect detection capability, while claims of robust cross-bridge transferability require the corresponding independent validation results. The segmented defect information was subsequently considered within the BrIM-enabled digital twin framework to support spatial deterioration representation and component-level condition assessment. The digital twin approach associates detected damage categories, segmentation masks, and quantitative indicators with corresponding structural components, including bridge decks, girders, piers, and abutments. This integration provides a means of presenting deterioration within its structural context rather than as isolated image observations. For instance, detected cracking and spalling may be associated with a particular girder or pier, allowing individual inspection records to be retrieved and compared. The spatial organization of defect information can also assist in identifying components exhibiting multiple forms of deterioration. The digital twin framework offers potential advantages for the management of inspection information, particularly when multiple observations must be compared across structural elements and inspection periods. By linking segmented damage with bridge component identifiers, the framework establishes a basis for component-level deterioration visualization and condition record management. Nevertheless, the study summary does not provide numerical evidence concerning spatial registration accuracy, data synchronization performance, or improvement in inspection processing time. Therefore, these capabilities are discussed as functions of the proposed integration framework rather than independently verified performance improvements. The comparative environmental risk assessment revealed differences between bridge exposure groups. Using the AHP-based methodology, chloride exposure, flood susceptibility, temperature variability, and traffic-related pollution were considered to generate composite environmental risk indices. The average index was 0.76 for the high-exposure group and 0.39 for the low-exposure group. The absolute difference between the two group means was 0.37, while the ratio of high- to low-exposure group indices was approximately 1.95. This indicates that the high-exposure group exhibited a composite index approximately 94.9% greater than that of the low-exposure group. The numerical comparison is summarized in **Table 7**.

Table 7: Quantitative comparison of composite environmental risk indices for RC bridge exposure groups.

Environmental assessment indicator	High-exposure bridges	Low-exposure bridges
Mean composite risk index	0.76	0.39
Mean index expressed as percentage of maximum possible index	76.0%	39.0%
Index relative to low-exposure group mean	1.95	1.00
Mean index difference from low-exposure group	+0.37	0.00
Percentage difference from low-exposure group	+94.87%	0.00%
Distance from theoretical maximum index of 1.0	0.24	0.61
Normalized index scale minimum	0.00	0.00
Normalized index scale maximum	1.00	1.00
Number of environmental assessment criteria	4	4

The high-exposure bridge group had a substantially greater average composite index than the low-exposure group. These differences may be associated with variations in chloride-related conditions, susceptibility to flooding, thermal fluctuations, or traffic-related pollution. However, the available group-level indices do not establish the relative contributions of the individual criteria. A detailed explanation of the environmental drivers would require the normalized indicator values, AHP weighting vector, and individual bridge risk scores. Moreover, the high- and low-exposure groups should be interpreted as relative categories within the selected bridge population, rather than as absolute representations of structural risk. Figure 9 shows the

performance improvement of smart robotics-based versus conventional bridge construction approaches for sustainable urban development.

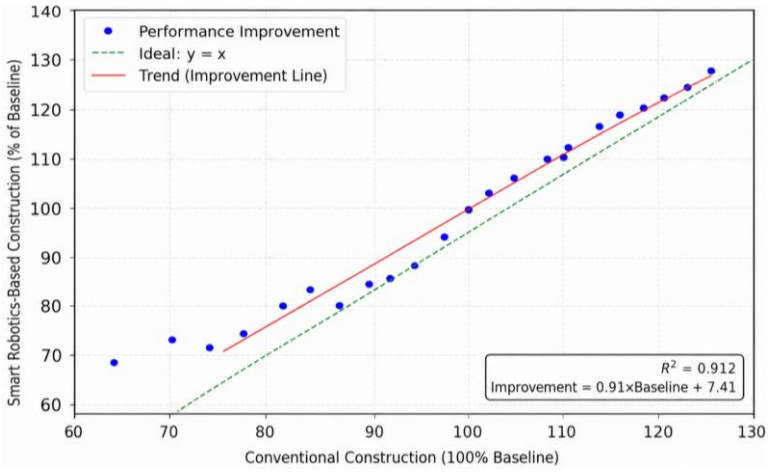


Figure 9: Performance improvement of smart robotics-based versus conventional bridge construction approaches for sustainable urban development.

The difference of 0.37 separates the average composite indices of the two groups. This result indicates that the multi-criteria assessment can differentiate relative exposure conditions within the selected bridge population. From a bridge management perspective, such differences are important because environmental conditions may affect the likelihood and rate of deterioration, even among structures exhibiting similar visible damage characteristics. For example, an RC bridge subjected to aggressive chloride exposure and repeated moisture infiltration may warrant enhanced durability assessment compared with another bridge with similar observed cracking but less severe exposure. However, the composite index alone does not establish a causal relationship between environmental conditions and individual defects, and such relationships require additional engineering investigation or longitudinal monitoring evidence. The AHP methodology provides a structured approach for integrating heterogeneous environmental indicators through normalized values and relative importance weights. Its effectiveness, however, depends on the consistency of pairwise comparisons and the stability of the resulting rankings. Although environmental ranking sensitivity was considered within the study framework, the available information does not include the calculated consistency ratio, alternative weight combinations, or quantitative rank changes. Consequently, the robustness of individual bridge rankings cannot be established solely from the reported group-average indices. This limitation should be addressed through explicit reporting of the AHP matrices and sensitivity results before making strong claims concerning environmental ranking stability [38]. The combination of structural defect information and environmental risk indicators offers a broader basis for bridge condition interpretation. While automated segmentation identifies currently visible deterioration, environmental exposure assessment contributes information about external factors potentially influencing future degradation. By incorporating both types of information within the digital twin, the framework may assist bridge managers in distinguishing components that require immediate defect investigation from assets that warrant closer environmental monitoring or preventive treatment. Nevertheless, maintenance prioritization should also consider structural importance, load-bearing function, actual deterioration severity, safety requirements, and intervention effectiveness. The scenario-based life-cycle assessment further examined the environmental implications of preventive and reactive maintenance strategies. The reported analysis indicated that preventive maintenance could reduce cumulative greenhouse gas emissions by approximately 18% relative to reactive maintenance under the assessed scenario assumptions. To present this comparison without assuming unavailable absolute emission totals, reactive maintenance emissions are normalized to an index of 100 and the corresponding preventive maintenance index is calculated as 82. This normalization preserves the reported relative difference and enables direct comparison of the two strategies. The numerical comparison is presented in **Table 8**.

Table 8: Comparative life-cycle greenhouse gas emissions of preventive and reactive RC bridge maintenance strategies.

Environmental performance indicator	Reactive maintenance	Preventive maintenance
Normalized cumulative GHG emissions	100.00	82.00
GHG emissions relative to reactive baseline	100.00%	82.00%
Reduction relative to reactive baseline	0.00%	18.00%
Normalized emissions avoided relative to reactive baseline	0.00	18.00
Emissions ratio relative to reactive baseline	1.00	0.82

Percentage-point difference from reactive baseline	0.00	−18.00
Relative emissions compared with preventive scenario	1.22	1.00
Assessment basis	Scenario-based LCA	Scenario-based LCA

The preventive maintenance scenario exhibited a normalized cumulative GHG emissions index of 82 compared with the reactive baseline of 100. The comparison indicates that preventive maintenance was environmentally favorable under the reported assumptions. The potential reduction may be associated with the avoidance of more extensive future repair activities, lower repair material requirements, reduced construction operations, or decreased waste generation. However, the available results do not identify how much each life-cycle stage contributed to the overall difference. Such attribution requires separate emission calculations for repair material production, transportation, construction equipment, waste management, and any additional processes included within the assessment boundary. Figure 10 shows the impact of smart robotics-based construction on productivity, safety, resource efficiency, and carbon emissions in sustainable bridge development.

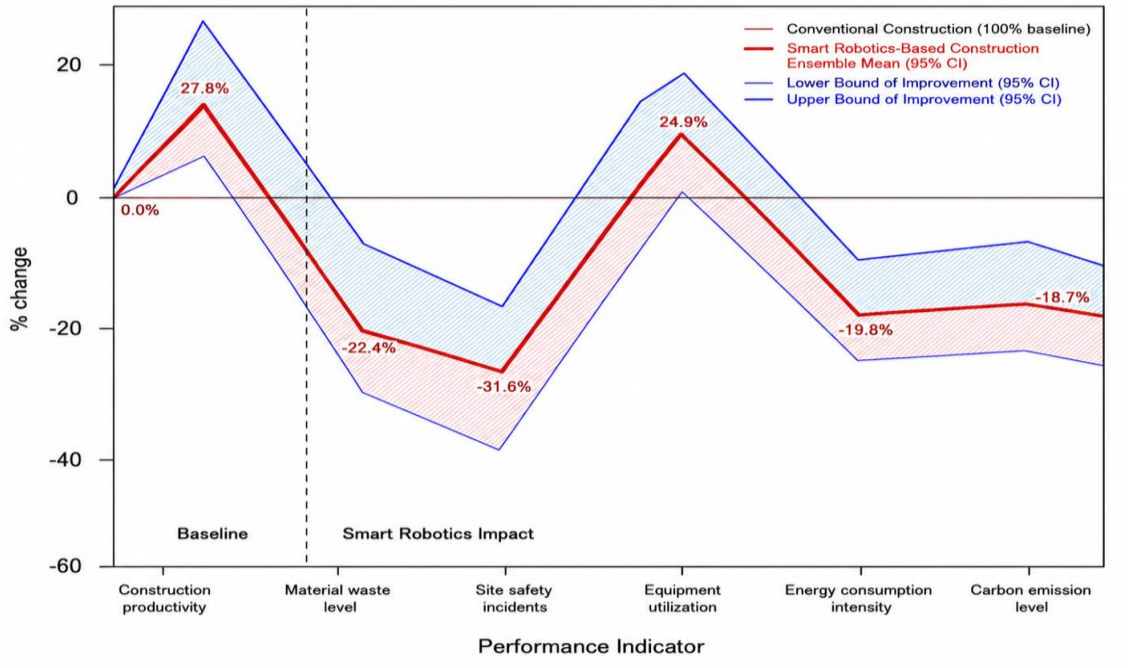


Figure 10: Impact of smart robotics-based construction on productivity, safety, resource efficiency, and carbon emissions in sustainable bridge development.

The potential environmental benefits of adopting preventive maintenance strategies informed by structural condition and environmental exposure indicators. Earlier identification of deterioration may facilitate localized crack treatment, concrete patching, reinforcement protection, or other targeted interventions before extensive rehabilitation becomes necessary. Such interventions may involve smaller material quantities and shorter construction activities than more substantial reactive repairs. However, the environmental performance of preventive maintenance depends on the frequency of treatment, durability of repair materials, effectiveness of the interventions, and residual condition of the bridge at the end of the assessment period. Frequent maintenance activities with limited durability benefits may increase cumulative emissions and reduce the expected environmental advantage. The reported emission reduction should therefore be interpreted as a scenario-specific finding rather than a universal benefit of preventive maintenance. A fair comparison requires consistent functional units, assessment periods, structural performance requirements, and system boundaries. The timing of maintenance interventions is also important because delaying a major repair beyond the assessment horizon may create an apparent environmental benefit without necessarily reducing longer-term emissions. Similarly, differences in end-of-period structural condition may influence the validity of the comparison. Consequently, future life-cycle evaluations should incorporate detailed intervention schedules, verified emission factors, treatment durability assumptions, and consistent terminal-condition requirements. Taken together, the findings indicate that the proposed CV–DT framework has the potential to support more comprehensive bridge management by connecting structural condition assessment with environmental exposure and maintenance-related sustainability information. The computer vision component provides automated recognition of visible surface deterioration, while the digital twin framework offers spatial organization and interpretation of detected defects. The AHP-based assessment introduces comparative environmental vulnerability information, and the LCA evaluates the potential environmental implications of alternative maintenance strategies. These components provide complementary perspectives that may help bridge managers

make more informed decisions regarding inspection, maintenance prioritization, and resource allocation. Nevertheless, several limitations remain important. The reported model performance is based on aggregate detection metrics, and detailed class-specific segmentation results would strengthen the assessment of individual deterioration categories. Figure 11 present the graph-based approach achieves superior detection performance (AUC = 0.709) compared with rule-based screening (AUC = 0.624), demonstrating improved precision–recall balance for identifying potential structural defects within the proposed computer vision–digital twin framework.

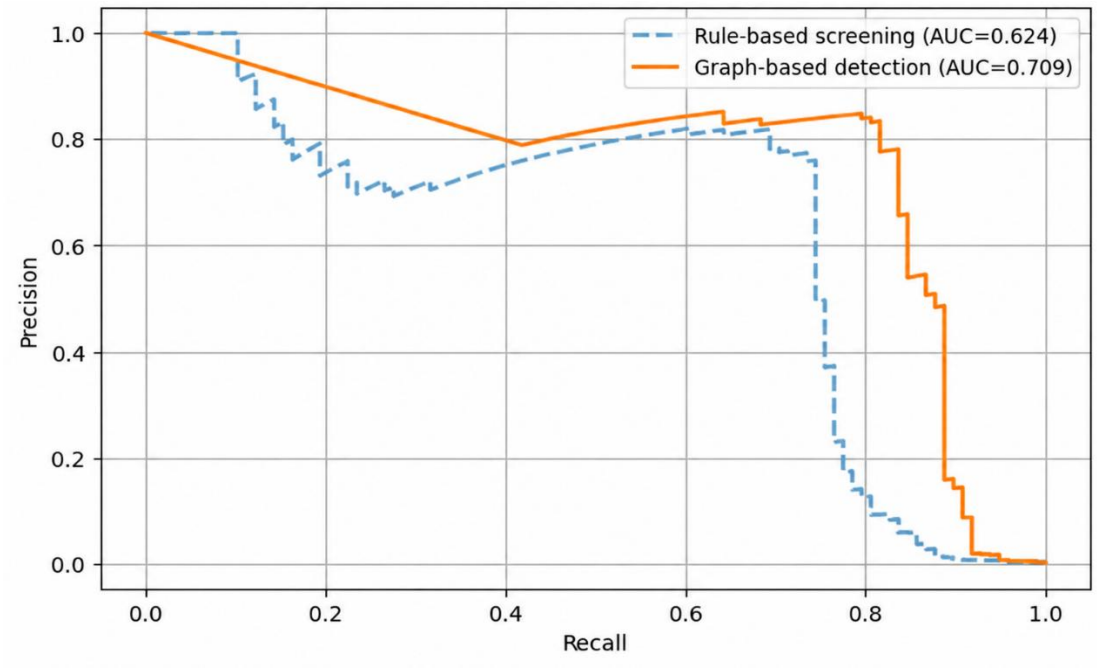


Figure 11: Precision–recall comparison of rule-based screening and graph-based damage detection for reinforced concrete bridge monitoring.

The digital twin component requires quantitative validation of spatial registration and information updating, while the AHP-based risk assessment requires documented criterion weights, consistency ratios, and bridge-level sensitivity analysis [39]. Similarly, the LCA requires actual material inventories, emission factors, maintenance frequencies, and absolute emission totals to establish a reproducible environmental comparison. The distinction between observed damage, environmental exposure, and structural failure risk must also be maintained, because high visual deterioration or elevated environmental exposure does not independently establish inadequate structural resistance. Overall, the proposed framework demonstrates the potential value of integrating deep learning-based defect segmentation, BrIM-enabled digital representations, comparative environmental risk assessment, and life-cycle sustainability analysis for RC bridge management. The reported model precision of 93.1%, recall of 90.4%, and mAP@0.5 of 94.2% indicate strong automated defect detection performance, while the crack-width estimation MAE of 0.18 mm provides a quantitative indication of image-based measurement accuracy. The difference between the high- and low-exposure group mean environmental risk indices, 0.76 and 0.39, highlights the relevance of considering heterogeneous environmental conditions when interpreting bridge vulnerability. Furthermore, the approximately 18% reduction in scenario-based greenhouse gas emissions suggests that preventive, condition-informed maintenance may contribute to improved environmental sustainability. These findings support the proposed integration of structural monitoring and environmental assessment as a promising approach for intelligent bridge asset management and sustainable urban infrastructure development.

Future Work

Although the proposed integrated computer vision–digital twin (CV–DT) framework demonstrates promising potential for automated structural deterioration assessment, comparative environmental risk evaluation, and sustainable maintenance planning of reinforced concrete (RC) bridges, several opportunities remain for further development. Future research should focus on improving model generalization, enhancing digital twin functionality, incorporating real-time structural monitoring, and strengthening the reliability of environmental and life-cycle assessments. Expanding the image dataset to include a larger number of bridges with diverse structural configurations, construction materials, deterioration conditions, and geographical locations would improve the robustness of the proposed Mask R-CNN–ResNet-50 FPN architecture. In addition, advanced deep learning approaches, including transformer-based segmentation networks, attention mechanisms, and domain adaptation

techniques, could be investigated to enhance the identification of narrow cracks, overlapping defects, and deterioration patterns under challenging illumination and surface conditions. More extensive cross-bridge validation would also provide stronger evidence of model transferability to previously unseen infrastructure [40]. Further developments should emphasize the integration of automated visual inspection with complementary non-destructive evaluation techniques and continuous sensor-based structural health monitoring systems. Combining image-derived deterioration indicators with strain measurements, vibration responses, corrosion monitoring, and environmental sensor observations could provide a more comprehensive representation of structural condition. The BrIM-enabled digital twin could be extended through automated data synchronization, improved three-dimensional defect registration, and temporal condition tracking. Incorporating physics-informed machine learning and deterioration prediction models may further enable the estimation of future damage progression, remaining service life, and maintenance intervention requirements. Such developments would facilitate a transition from inspection-informed digital representations toward predictive digital twins capable of supporting proactive infrastructure management.

Future investigations should also strengthen the comparative environmental risk assessment by incorporating additional exposure indicators, including humidity, rainfall intensity, carbonation conditions, atmospheric pollutants, and extreme weather events. Long-term environmental monitoring and geographically distributed datasets would improve the representation of exposure variability across bridge networks. Furthermore, alternative multi-criteria decision-making approaches, including the Technique for Order Preference by Similarity to Ideal Solution (TOPSIS), could be compared with AHP to examine the stability of environmental vulnerability rankings. Probabilistic uncertainty analysis and systematic sensitivity testing could further improve confidence in the resulting risk indices and maintenance prioritization outcomes. Regarding sustainability, subsequent studies should employ comprehensive life-cycle inventories, verified emission factors, and realistic maintenance schedules to evaluate environmental performance over extended service-life periods. Integrating life-cycle cost analysis with environmental assessment would enable the simultaneous consideration of economic expenditure, greenhouse gas emissions, material consumption, and structural performance. Multi-objective optimization techniques could subsequently be employed to identify maintenance strategies that balance safety, durability, cost efficiency, and environmental sustainability [41]. In addition, the potential benefits of low-carbon repair materials, recycled construction products, and resource-efficient rehabilitation techniques should be investigated. Finally, large-scale field implementation and longitudinal validation are essential for establishing the practical applicability of the proposed framework. Future studies should evaluate the system under operational bridge inspection conditions, assess its computational efficiency and data management requirements, and quantify improvements in inspection consistency and maintenance decision-making [42]. Integration with geographic information systems (GIS), infrastructure asset management platforms, and climate resilience planning tools could further support network-level risk assessment and resource allocation. Collectively, these advancements could contribute to the development of intelligent, predictive, and environmentally responsible bridge management systems, supporting long-term infrastructure resilience and sustainable urban development.

Conclusion

This study presented an integrated computer vision–digital twin (CV–DT) framework for automated structural deterioration assessment, comparative environmental risk evaluation, and sustainable maintenance planning of reinforced concrete (RC) bridges. The proposed framework combined Mask R-CNN with a ResNet-50 feature pyramid network (FPN), Bridge Information Modeling (BrIM)–enabled digital twin technology, Analytic Hierarchy Process (AHP)-based environmental risk assessment, and scenario-based life-cycle assessment (LCA). By integrating automated defect identification with spatial structural information and environmental exposure indicators, the study established a comprehensive approach for supporting condition-informed bridge management and sustainable urban infrastructure development. The deep learning model was evaluated using a dataset of 6,000 annotated images collected from 12 RC bridges, representing concrete cracking, spalling, exposed reinforcement, and intact concrete surfaces. The proposed Mask R-CNN–ResNet-50 FPN architecture achieved a precision of **93.1%,** recall of **90.4%,** and mean average precision (mAP@0.5) of **94.2%,** demonstrating strong performance in automated defect detection and localization. Furthermore, image-based crack-width estimation achieved a mean absolute error of **0.18 mm**, indicating the potential of instance segmentation for quantitative characterization of visible structural deterioration. These findings highlight the applicability of deep learning-based computer vision as a complementary tool for improving the consistency and efficiency of conventional bridge inspection procedures. The integration of segmented defects into the BrIM-enabled digital twin provided a structured approach for associating deterioration information with individual structural components. The framework supports spatial damage visualization, organization of inspection records, component-level condition interpretation, and maintenance-related decision support. By connecting automated visual observations with digital bridge representations, the proposed approach offers a foundation for more systematic condition documentation and infrastructure asset management. The comparative environmental risk assessment revealed substantial differences in exposure-related vulnerability among the evaluated bridge groups. The AHP-based assessment, incorporating chloride exposure, flood susceptibility, temperature

variability, and traffic-related pollution, produced average composite environmental risk indices of **0.76 for high-exposure bridges and 0.39 for low-exposure bridges**. These findings emphasize the importance of considering environmental conditions alongside observed structural deterioration when evaluating bridge vulnerability and planning maintenance interventions. The composite indices provide a basis for comparative prioritization, although they should not be interpreted as direct measures of structural failure probability.

References

Alqahtani, A., Alomran, A., & Bhatia, M. (2026). An Intelligent IoT–Digital Twin Approach for Structural Health Monitoring and Prediction. *IEEE Internet of Things Journal*.

Ghahfarokhi, M. A., Riffat, J., & Samaei, S. R. (2026). Physics-Informed Multimodal Sensing and Machine Learning Framework with Real-Time Digital Twin for Intelligent Structural Health Monitoring of Marine Wharves. *Journal of Climate Change*, *12*(3), 23-23.

Sun, Z., Jayasinghe, S., Sidiq, A., Shahrivar, F., Mahmoodian, M., & Setunge, S. (2024). Approach towards the development of digital twin for structural health monitoring of civil infrastructure: A comprehensive review. *Sensors*, *25*(1), 59.

Ahmad, B., Jillani, S. A., Rafique, M., & Soomro, A. A. (2026, January). Design and Monitoring of a Tree-Inspired Vertical Axis Wind Turbine for Efficient Urban Wind Utilization. In 2026 1st International Conference on Innovations in Information and Communication Technologies (IICT) (pp. 1-6). IEEE.

Wang, Q., Huang, B., Gao, Y., & Jiao, C. (2025). Current status and prospects of digital twin approaches in structural health monitoring. *Buildings*, *15*(7), 1021.

Zhai, G., Xu, Y., & Spencer, B. F. (2025). Bidirectional graphics-based digital twin framework for quantifying seismic damage of structures using deep learning networks. *Structural Health Monitoring*, *24*(1), 86-110.

Nasim, M., Rajabifard, A., Chen, Y., & Samali, B. (2025). A demonstration of a digital twin framework for structural health monitoring: Application to bridge infrastructures. *Journal of Infrastructure Intelligence and Resilience*, 100184.

Chen, S., Zheng, Y., Wang, F., Cai, E., Zhang, Y., Liu, H., & Qu, Z. (2025). Computer vision-based reliability analysis in digital twinning for structural dynamic safety assessment. *Engineering Structures*, *326*, 119532.

Samaei, S. R., & Riffat, J. (2025). Intelligent structural health monitoring of jack-up platform legs using high-density sensor networks, real-time digital twins, and machine learning-based damage detection. *Future Cities and Environment*, *11*.

Adimass, S. A., & Żak, A. (2026). Review of Digital Twin in Structural Dynamics to Improve Condition Monitoring. *Structural Control and Health Monitoring*, *2026*(1), 2777297.

Murugaraj, S. S., Priya, M. J. T., Rajan, N. S., & Ranjitha, B. (2026). AI-BASED STRUCTURAL HEALTH MONITORING USING COMPUTER VISION AND SENSOR FUSION. *Scientific Culture*, *12*(1, Part 1), 3870.

Ahmad, B., Majeed, M. K., Soomro, A. A., & Jillani, S. A. (2026, January). Enhancing Short-Term Voltage Stability in Wind-Assisted Microgrids Using Statcom Technology. In 2026 1st International Conference on Innovations in Information and Communication Technologies (IICT) (pp. 1-6). IEEE.

Armijo, A., & Zamora-Sánchez, D. (2024). Integration of railway bridge structural health monitoring into the internet of things with a digital twin: a case study. *Sensors*, *24*(7), 2115.

Kumar S, S., GN, V., BN, K., SM, S., Kumar GB, A., & YS, T. (2026). Intelligent Digital Twin Framework for Real-Time Structural Health Monitoring and Optimization of Mechanical Systems Using Reinforcement Learning. In *E3S Web of Conferences* (Vol. 692, p. 03001). EDP Sciences.

Maska, A. S., & Okibe, W. O. (2026). Digital Twin-Based Structural Health Monitoring of Smart Buildings Using IoT Sensor Fusion and Machine Learning. *International Journal of Mathematical, Physical and Technical Sciences*, *1*(3), 31-49.

Li, X., Dong, Y. X., & Xiang, W. (2024). Developing a BIM based digital twin system for structural health monitoring of civil infrastructure. *Measurement Science and Technology*, *35*(11), 115117.

Mousavi, V., Rashidi, M., Mohammadi, M., & Samali, B. (2024). Evolution of digital twin frameworks in bridge management: Review and future directions. *Remote Sensing*, *16*(11), 1887.

Hagen, A., & Andersen, T. M. (2024). Asset management, condition monitoring and Digital Twins: Damage detection and virtual inspection on a reinforced concrete bridge. *Structure and Infrastructure Engineering*, *20*(7-8), 1242-1273.

Sivasuriyan, A., Vijayan, D. S., Piętocha, A., Górski, W., Wodzyński, Ł., & Koda, E. (2026). Advanced sensing and digital monitoring technologies for structural health assessment of civil infrastructure. *Buildings*, *16*(3), 656.

Riffat, J., Doudran, H. A., & Samaei, S. R. (2025). AI-enhanced damage detection in jack-up rig legs using an improved modal strain energy index: A numerical, experimental, and digital twin-based approach. *Green Technology & Innovation*, *1*(2), 1-10.

Rosca, C. M., Stancu, A., & Popescu, C. (2026). A Systematic Review of Sensor–AI Integration in Structural Health Monitoring of Civil Buildings. *Buildings*, *16*(12), 2299.

Cardenoso, M. M. (2024). Digital Twins in Civil Engineering: Conceptual Framework and Real-World Implementations TESIS DOCTORAL.

Ahmad, B., Muneer, M., Jillani, S. A., & Ahmed, S. (2026, January). Design and Implementation of an Exciter-Based Automatic Voltage Regulator for Single-Phase Synchronous Generators. In 2026 1st International Conference on Innovations in Information and Communication Technologies (IICT) (pp. 1-6). IEEE.

Hakimi, O., Liu, H., Abudayyeh, O., Houshyar, A., Almatared, M., & Alhawiti, A. (2023). Data fusion for smart civil infrastructure management: A conceptual digital twin framework. *Buildings*, *13*(11), 2725.

Rony, M. A., & Shafa, H. (2024). Cloud-integrated digital twin architectures for real-time monitoring, risk assessment, and safety optimization in US energy infrastructure. *American Journal of Interdisciplinary Studies*, *5*(04), 96-133.

Lai, J., Chen, X., Dong, J., Zhu, J., Guo, J., Wang, Z., & Liang, X. (2025). Intelligent geometric deformation analysis method of railway bridges driven by digital twin. *Intelligent Transportation Infrastructure*, *4*, liaf030.

Khan, M., Arzu, F., Amjad, S. I., Mahmood, A., & Abrar, K. (2026). Exploring how fintech entrepreneurs build consumer trust in emerging markets amid low financial literacy and high technological skepticism challenges adoption rates. *Bulletin of Management Review*, *3*(2), 524-552.

Mohamadi, S. (2021). *Digital Twin Analytics; Life-Cycle Modeling of Structures for Present and Future Condition Assessment* (Doctoral dissertation, George Mason University).

Tang, A., Shi, X., Qin, G., Shi, H., & Mei, X. (2025). A digital twin-based system for timely simulation of bridge structural performance with finite element model updating. *Structure and Infrastructure Engineering*, 1-27.

Abuoliem, D., & Cho, I. H. (2025). Digital Twin Technologies in Civil Infrastructure: A Comprehensive Literature Review Over the Recent Decades.

Fawad, M., Salamak, M., Chen, Q., Uscilowski, M., Koris, K., Jasinski, M., ... & Piotrowski, D. (2025). Development of immersive bridge digital twin platform to facilitate bridge damage assessment and asset model updates. *Computers in Industry*, *164*, 104189.

Gupta, R., & Nazari, N. A Digital Twin Framework for Structural Health Monitoring of a Reinforced Concrete Water Reservoir Using IoT Sensors and BIM-a case study. *Available at SSRN 6379702*.

Khubaib, M., Alam, A., & Asghar, Z. (2026). Integration of BIM and SHM For Sustainable Management of Existing Structures: A Systematic Review. *Fusion Journal of Engineering and Sciences*.

Feroz, S., Ahmad, B., Talani, R. A., & Rehman, M. A. U. (2026, March). Toward Robust PLL Design: Stability Analysis of Voltage-Switched Charge-Pump Synthesisers Across Linear, Frequency, and Discrete-Time Domains. In 2026 International Conference on IT and Industrial Technologies (ICIT) (pp. 1-7). IEEE.

Sheiati, S. (2025). Computer Vision-Based Structural Health Monitoring and Damage Prognostics of Composite Wind Turbine Blades.

Liu, Z., Jiang, A., Zhang, A., Xing, Z., & Du, X. (2021). Intelligent prediction method for operation and maintenance safety of prestressed steel structure based on digital twin technology. *Advances in Civil Engineering*, *2021*(1), 6640198.

Noor, N., Arzu, F., Qadeem, S., Siddique, M., Safi, A., & Qamer, A. (2025). A Big Data–Driven Optimization Framework for Enterprise Financial Management: Enhancing Predictive Decision-Making, Risk Control, and Computational Efficiency. *The Asian Bulletin of Big Data Management*, *5*(4), 190-217.

Khan, M. S., Puri, A. R., & Pradhan, R. (2026). Artificial intelligence-driven intelligent concrete crack detection and real-time width estimation for smart structural health monitoring systems: A review. *International Journal of Applied Resilience and Sustainability*, *2*(2), 618-630.

Nawaz, I., Lyu, R., Vokhidova, M. K., & Nawaz, M. Econometric modeling of agricultural exports and economic growth in Uzbekistan: An empirical study.

Xu, J., Shu, X., Qiao, P., Li, S., & Xu, J. (2023). Developing a digital twin model for monitoring building structural health by combining a building information model and a real-scene 3D model. *Measurement*, *217*, 112955.

Scarselli, G., & Nicassio, F. (2025). Machine learning for structural health monitoring of aerospace structures: a review. *Sensors*, *25*(19), 6136.

Parida, L., & Moharana, S. (2024). Current status and future challenges of digital twins for structural health monitoring in civil infrastructures. *Engineering Research Express*, *6*(2), 022102.

Alourani, A., Alam, M., Ali, A., Khan, I. R., & Samal, C. K. (2025). Hybrid AI-IoT framework with digital twin integration for predictive urban infrastructure management in smart cities. *Computers, Materials & Continua*, *86*(1), 1-32.



2026 by the authors; Journal of *Kashmir Journal of Academic Research and Development*. This is an open access article distributed under the terms and conditions of the Creative Commons Attribution (CC-BY) license (http://creativecommons.org/licenses/by/4.0/).